

Evaluation and Projection of Surface PM_{2.5} and Its Exposure on Population in Asia Based on the CMIP6 GCMs

Ying Xu^{1, 2, *}, Jie Wu³, Zhen-Yu Han^{1, 2}

¹ National Climate Center, China Meteorological Administration, Beijing 100081, China

² Laboratory for Climate Studies, China Meteorological Administration, Beijing 100081, China

³ School of Geography and Environmental Engineering, Gannan Normal University, Ganzhou 341000, China

14 Supplementary figures

Submitted to *International Journal of Environmental Research and Public Health*

July 22, 2022

Corresponding author:

Dr. Ying Xu, Email: xuying@cma.gov.cn

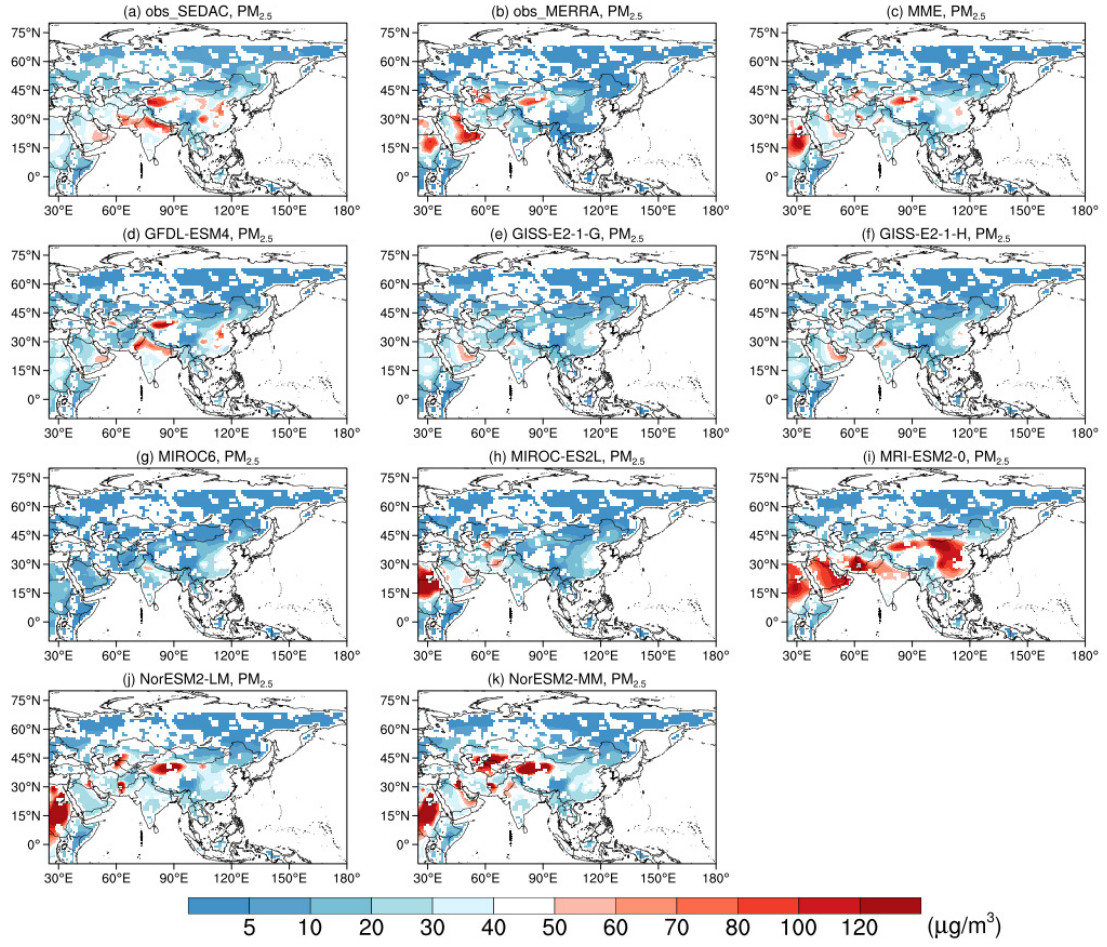


Figure S1. Spatial distribution of annual mean surface $PM_{2.5}$ concentrations (units: $\mu g/m^3$) during 1998-2014 from the observations, the original outputs of CMIP6 models and their bias.

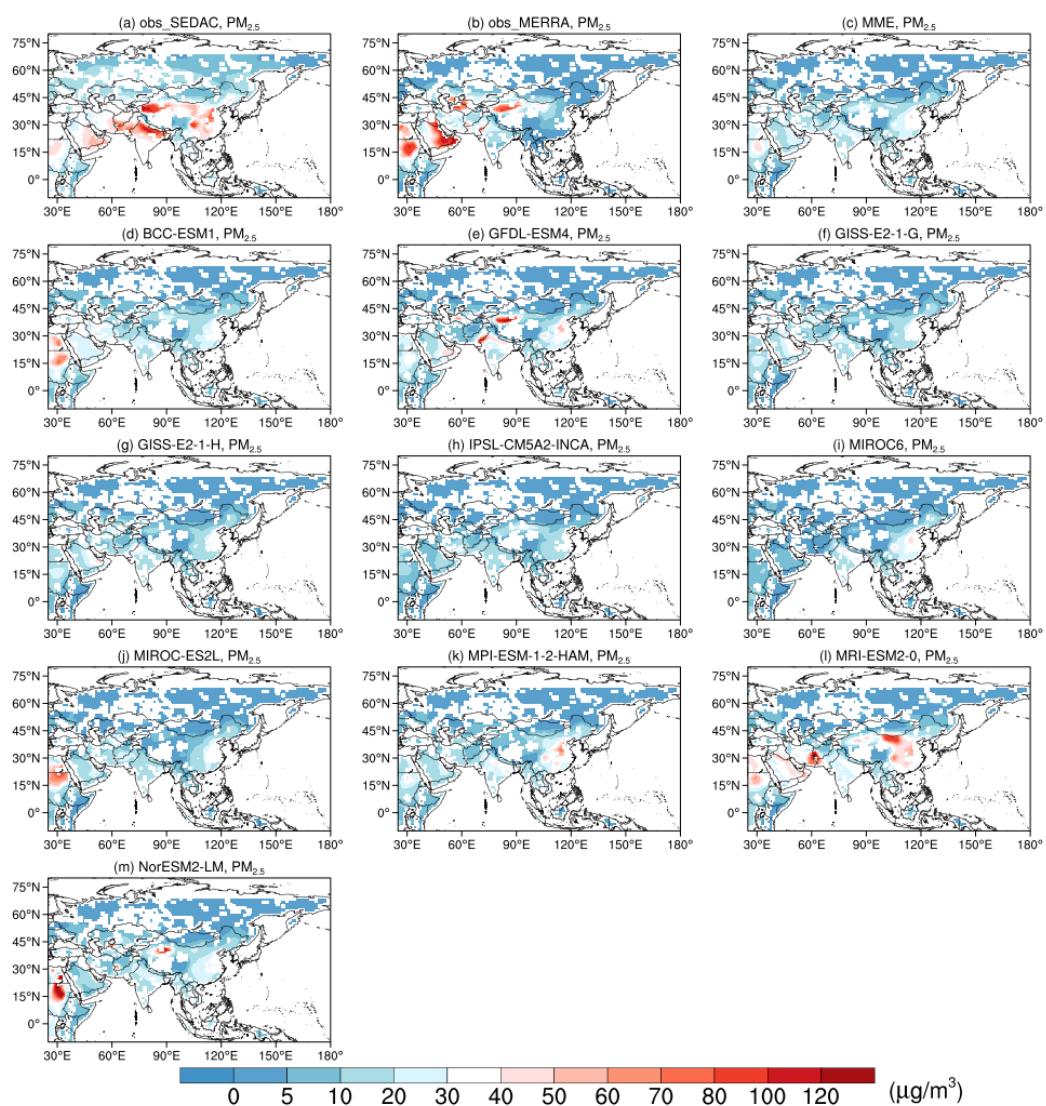
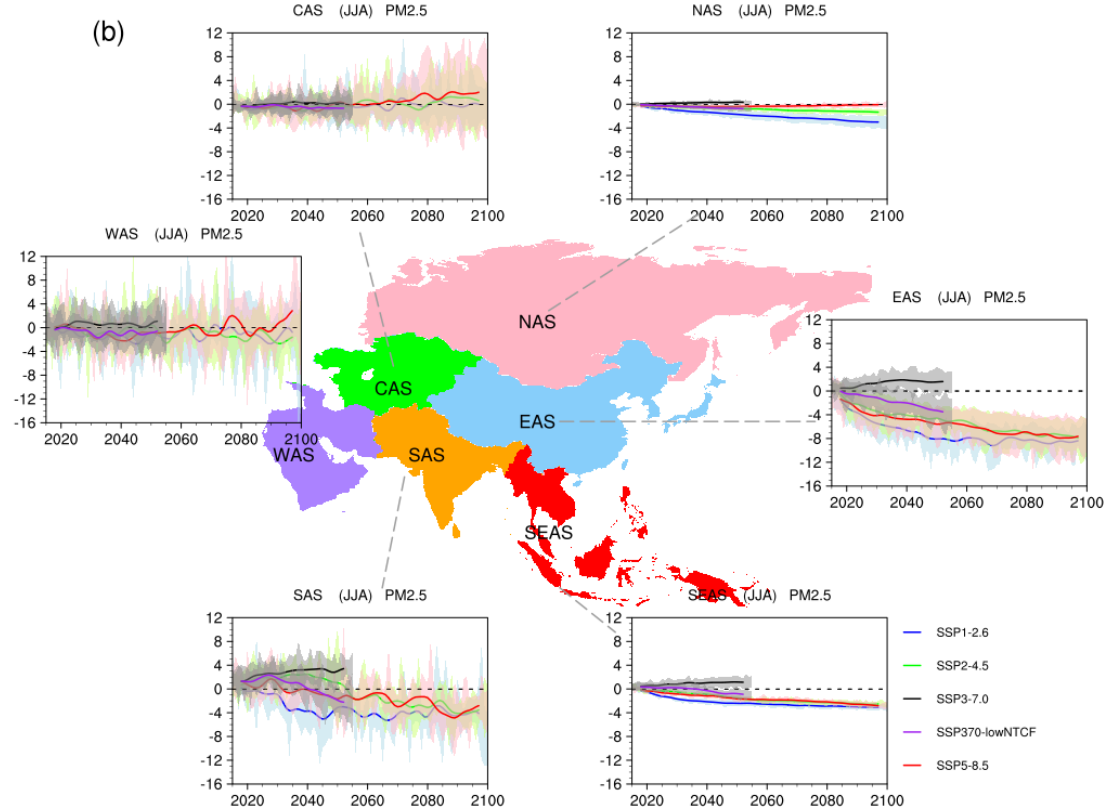
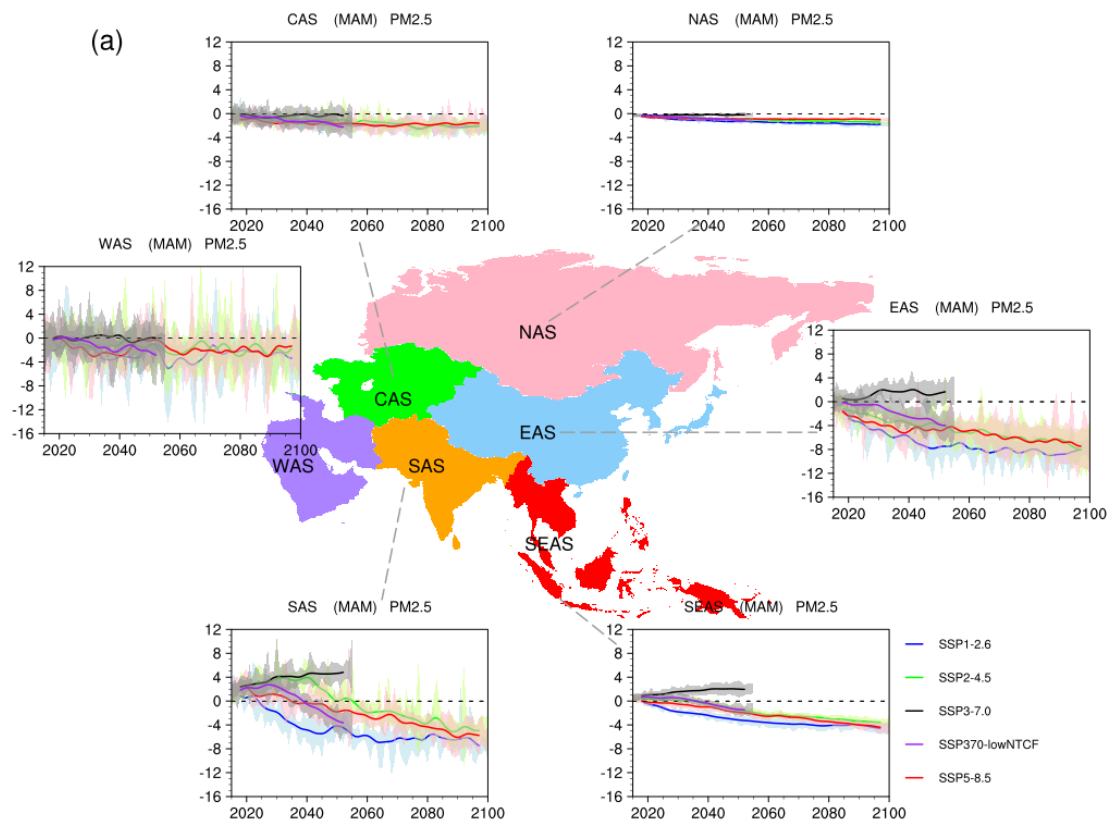


Figure S2. Same as Figure S1, but for the estimated.



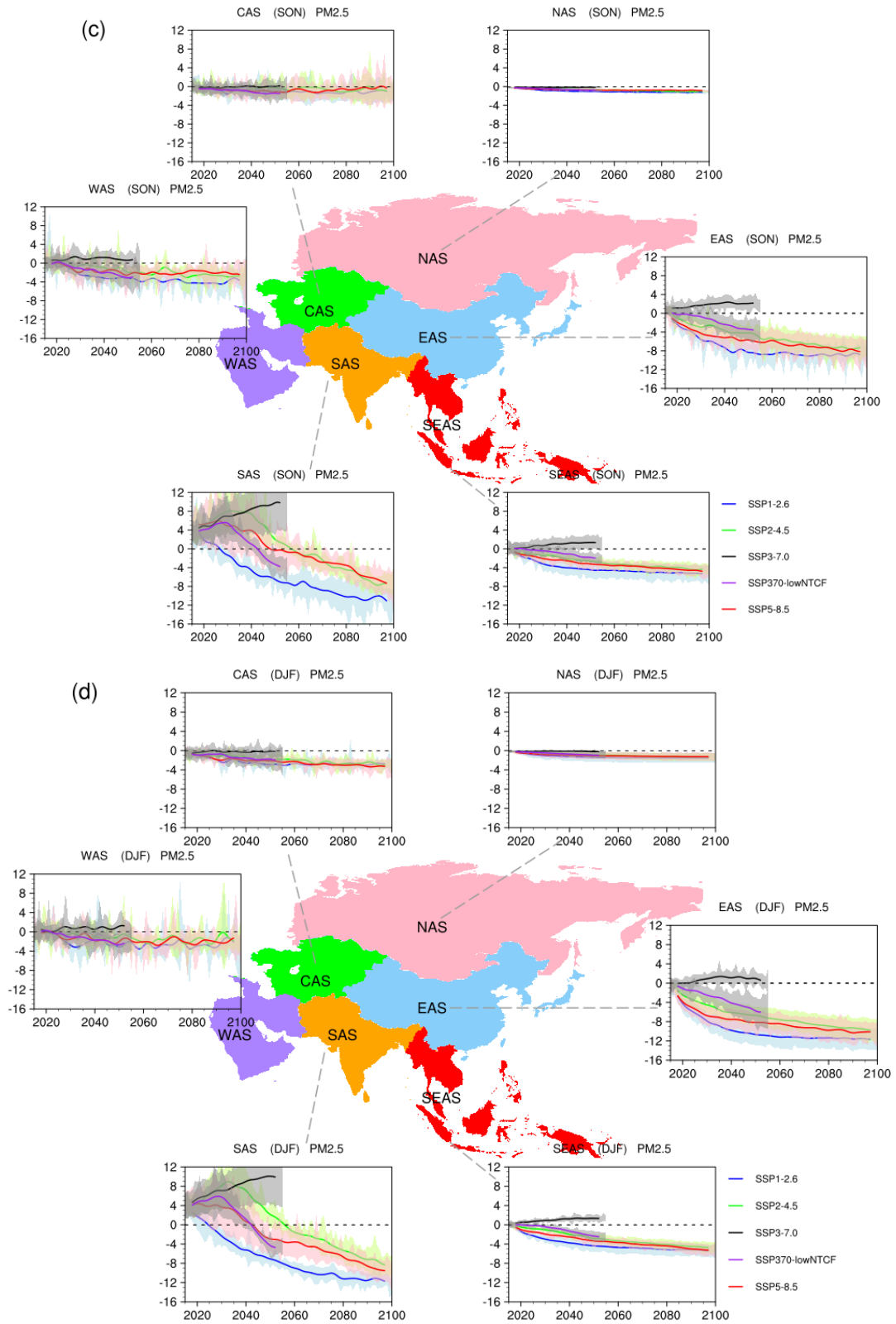
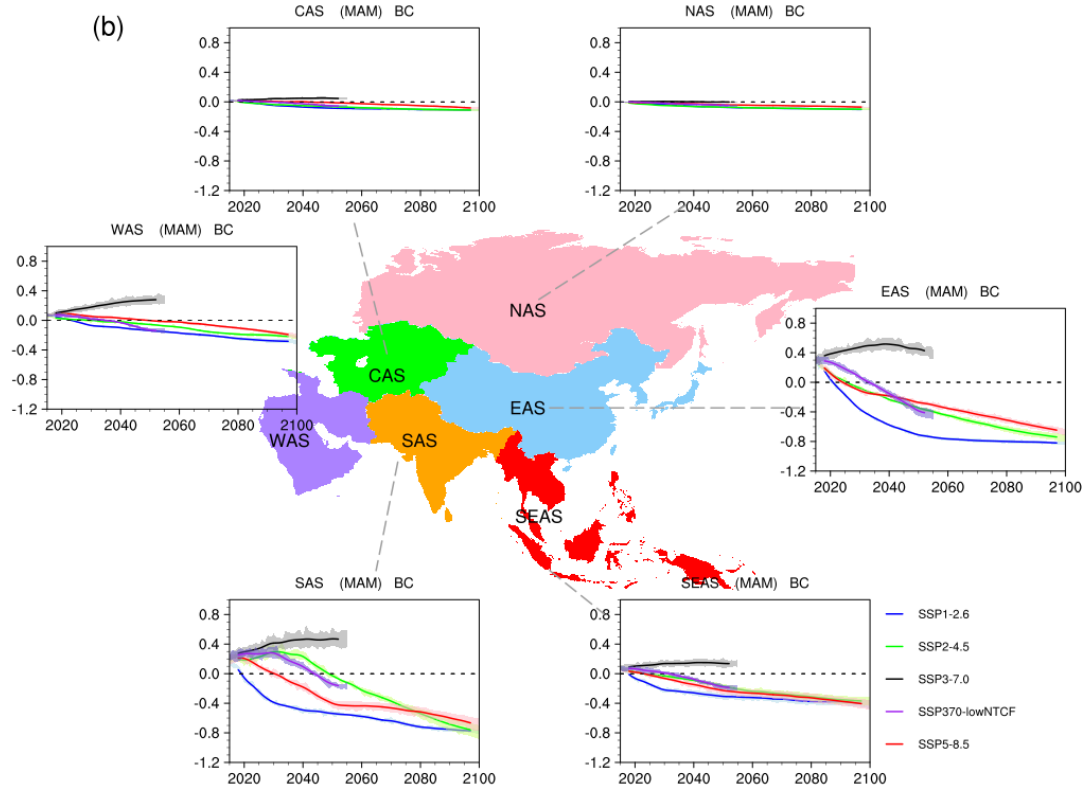
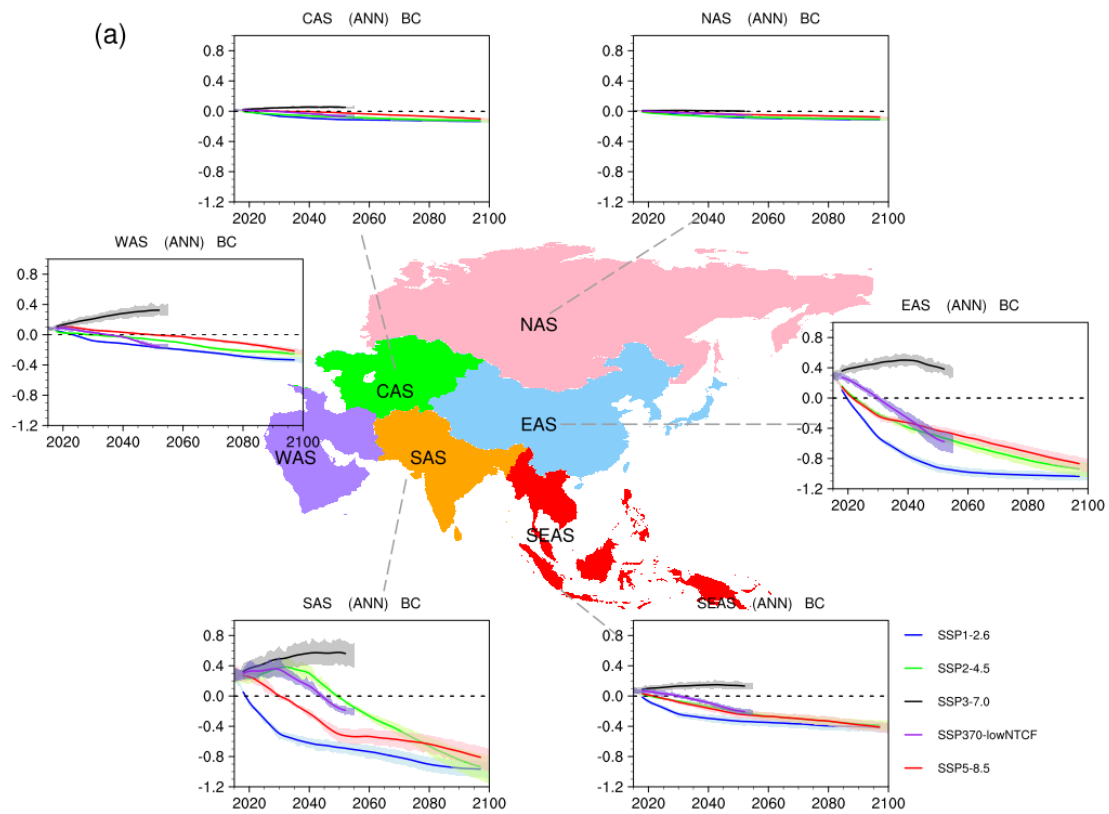
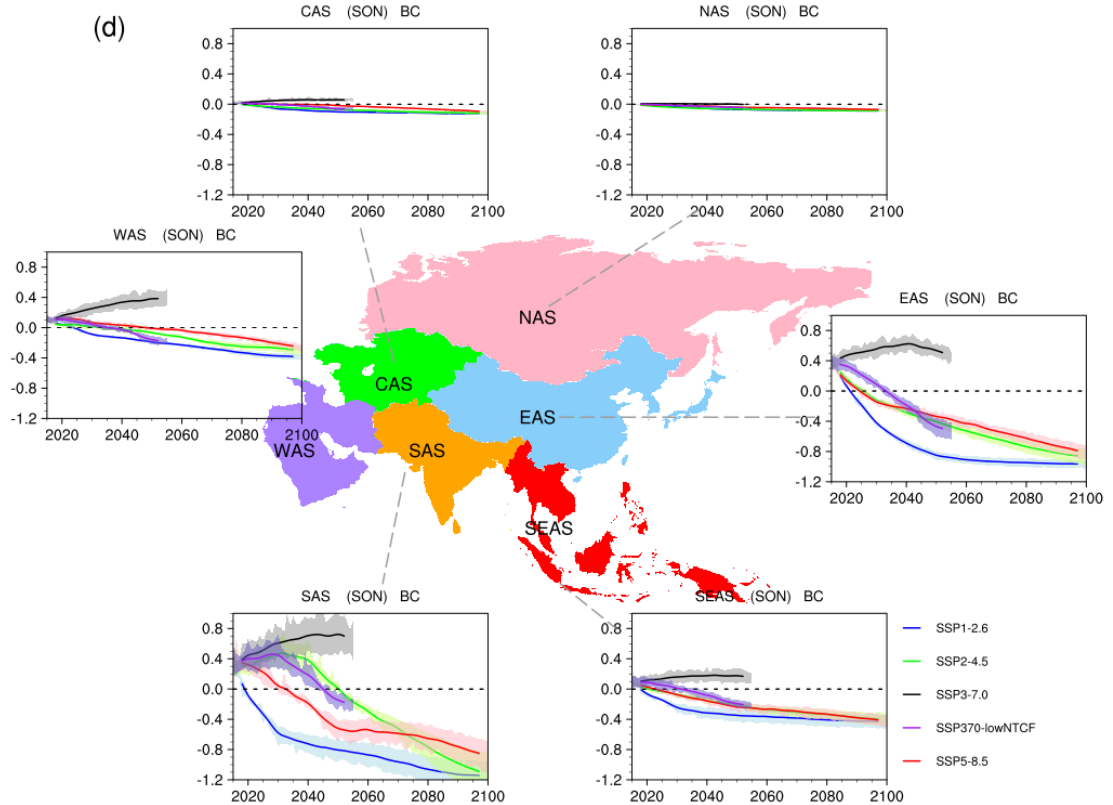
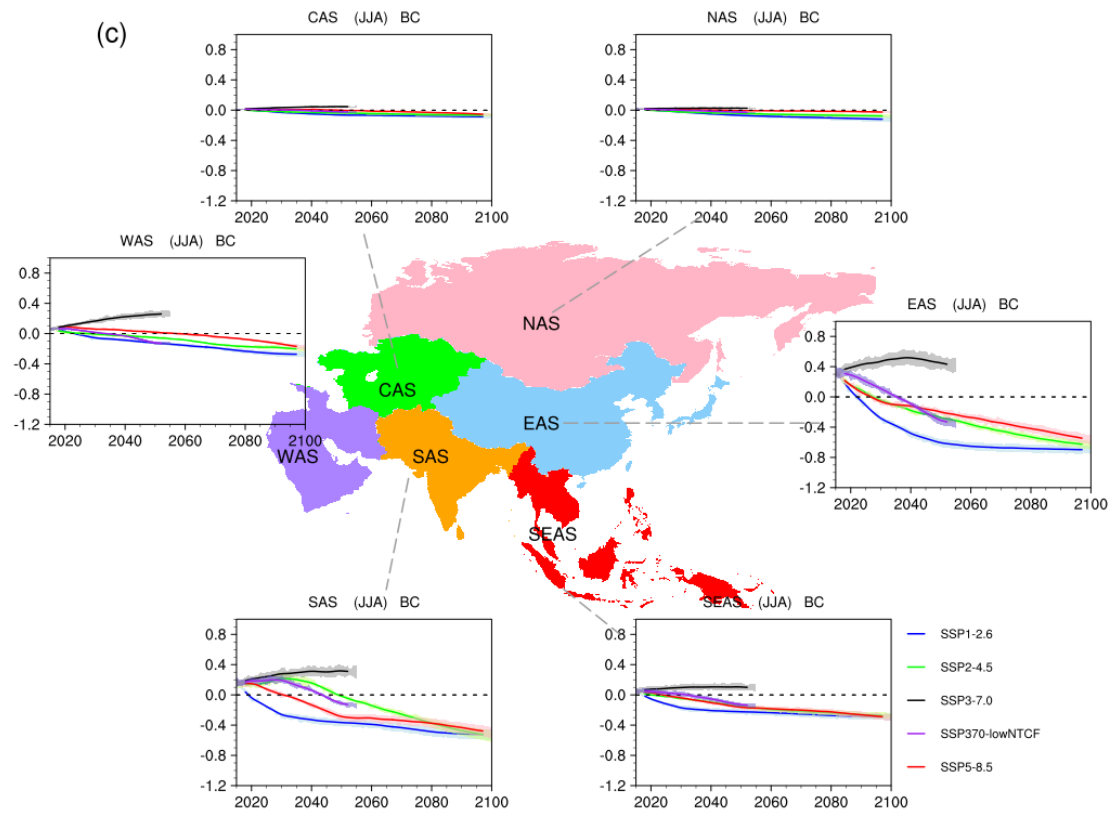


Figure S3 Time evolutions of surface $PM_{2.5}$ concentrations (units: $\mu g/m^3$) in spring(a), summer (b), autumn (c) and winter (d) over Asia under SSP1-2.6 (red curves), SSP2-4.5 (green curves), SSP3-7.0 (black curves), SSP370-lowNTCF (purple curves) and SSP5-8.5 (red curves), relative to 1995-2014, where shadings indicate model uncertainty range (1 standard deviation of the simulations).





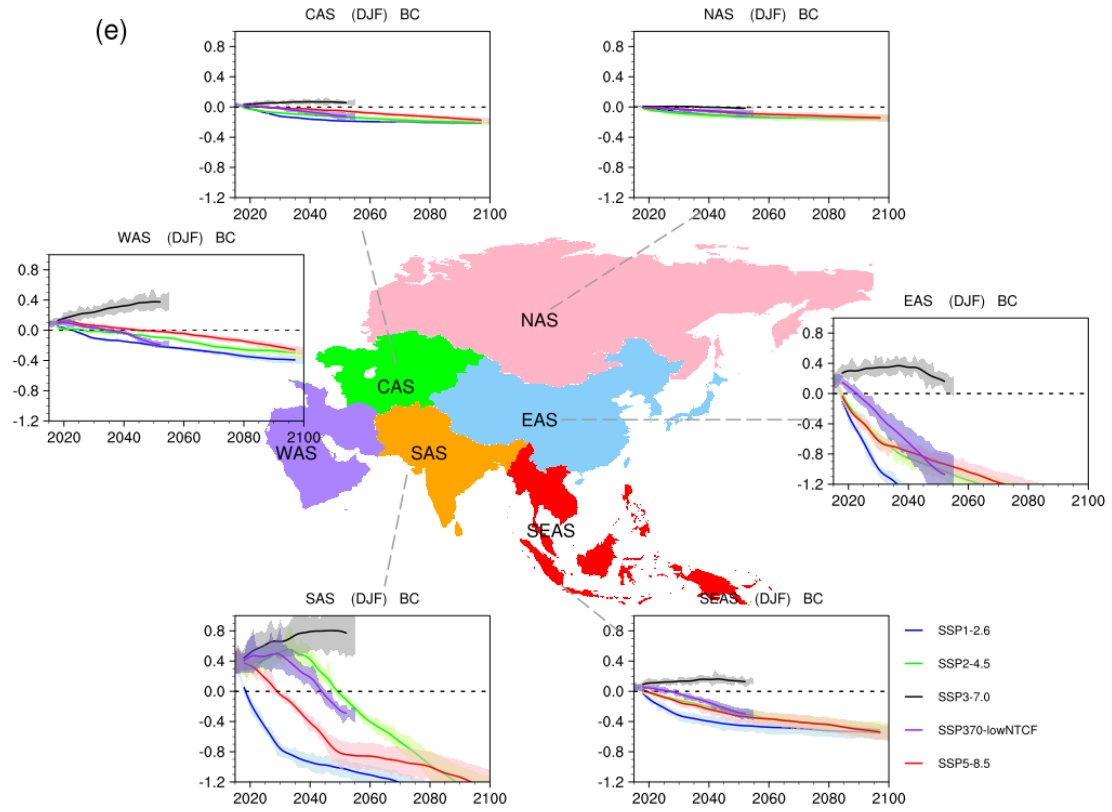
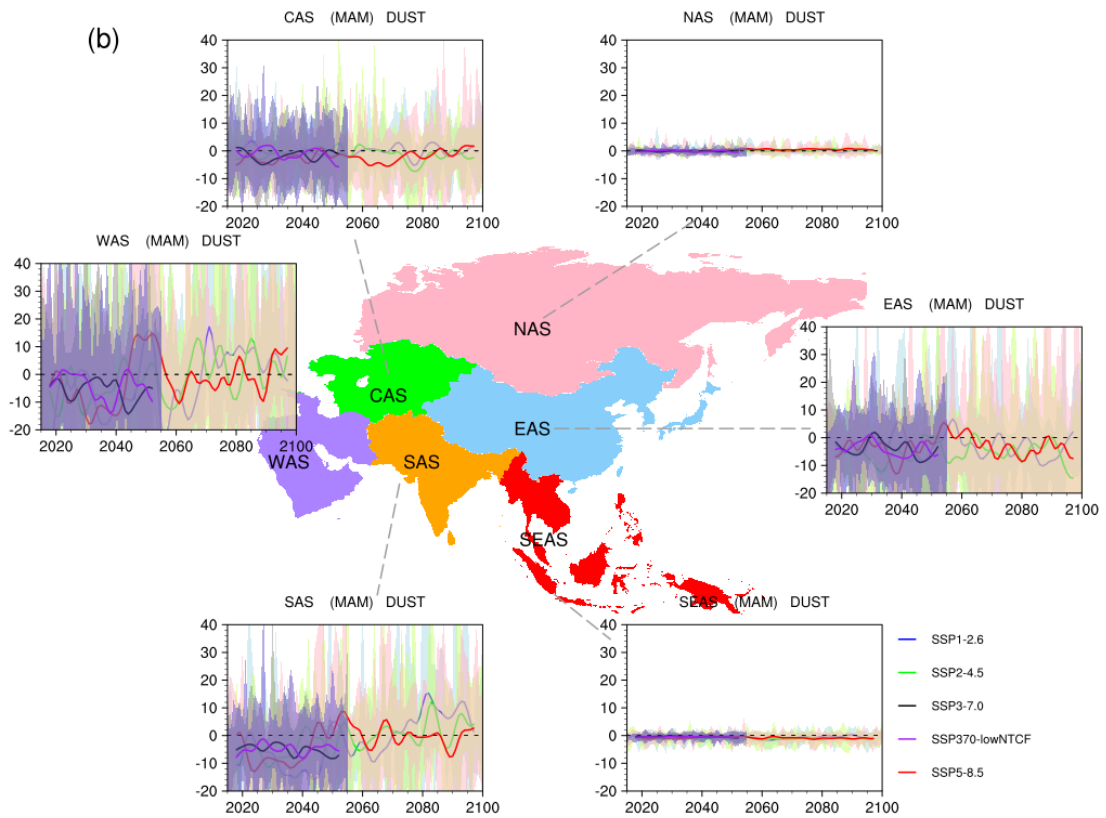
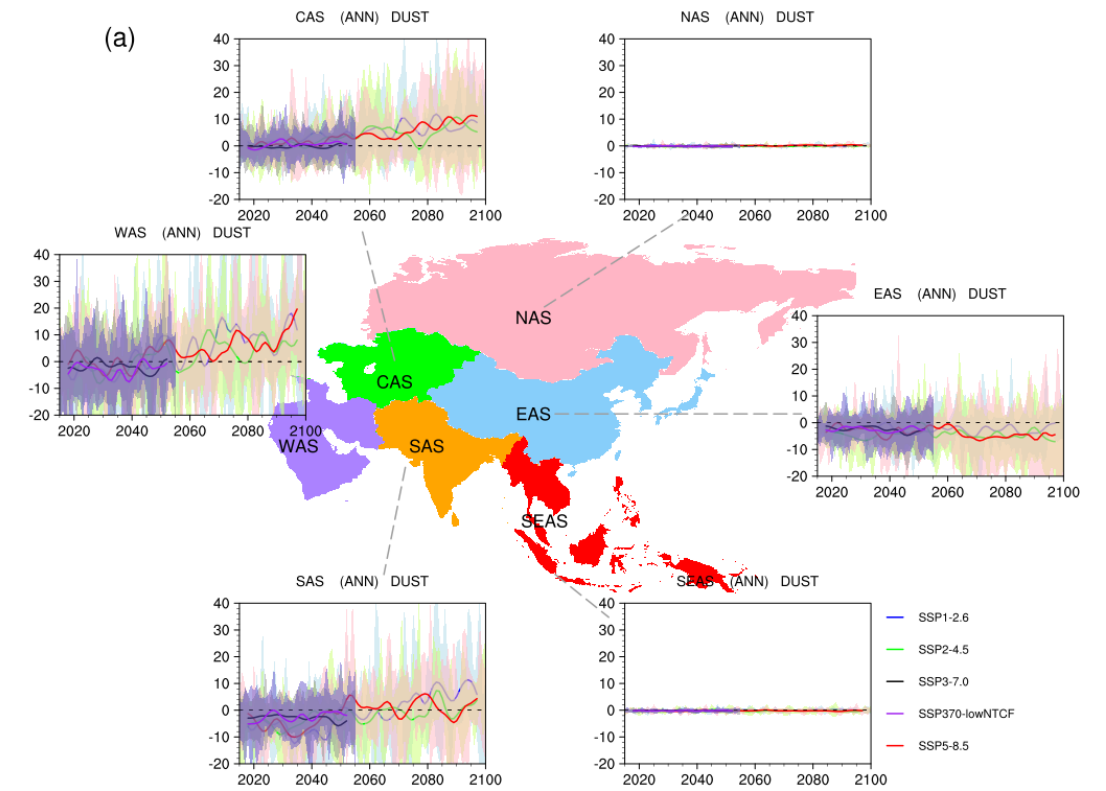
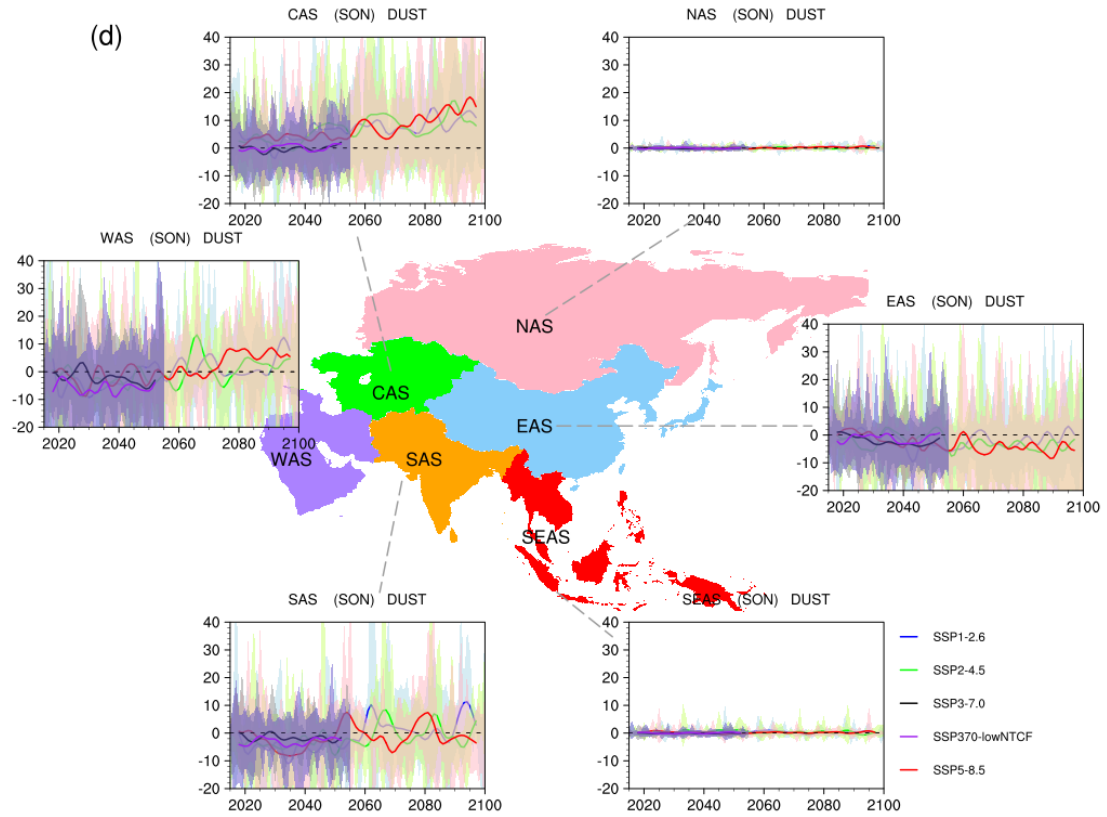
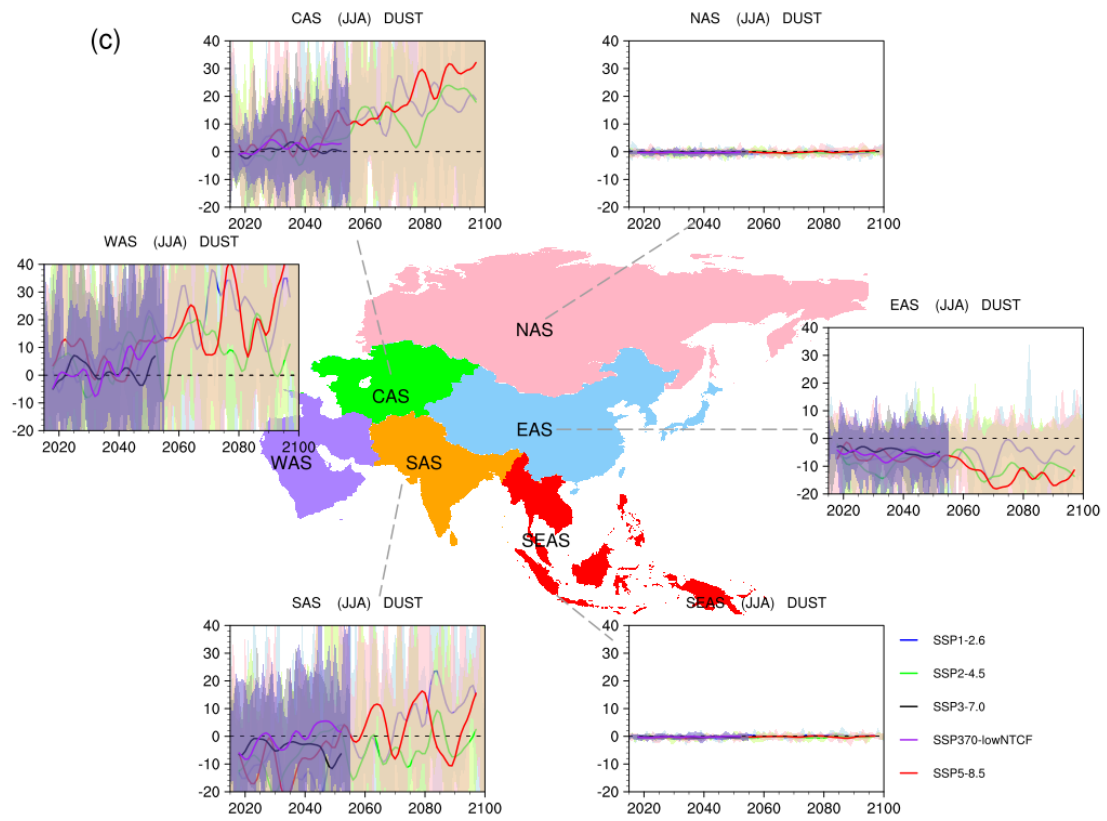


Figure S4 Time evolutions of surface black carbon (BC) concentrations (units: $\mu\text{g}/\text{m}^3$) in annual (a), spring (b), summer (c), autumn (d) and winter (e) over Asia under SSP1-2.6 (red curves), SSP2-4.5 (green curves), SSP3-7.0 (black curves), SSP370-lowNTCF (purple curves) and SSP5-8.5 (red curves), relative to 1995-2014, where shadings indicate model uncertainty range (1 standard deviation of the simulations).





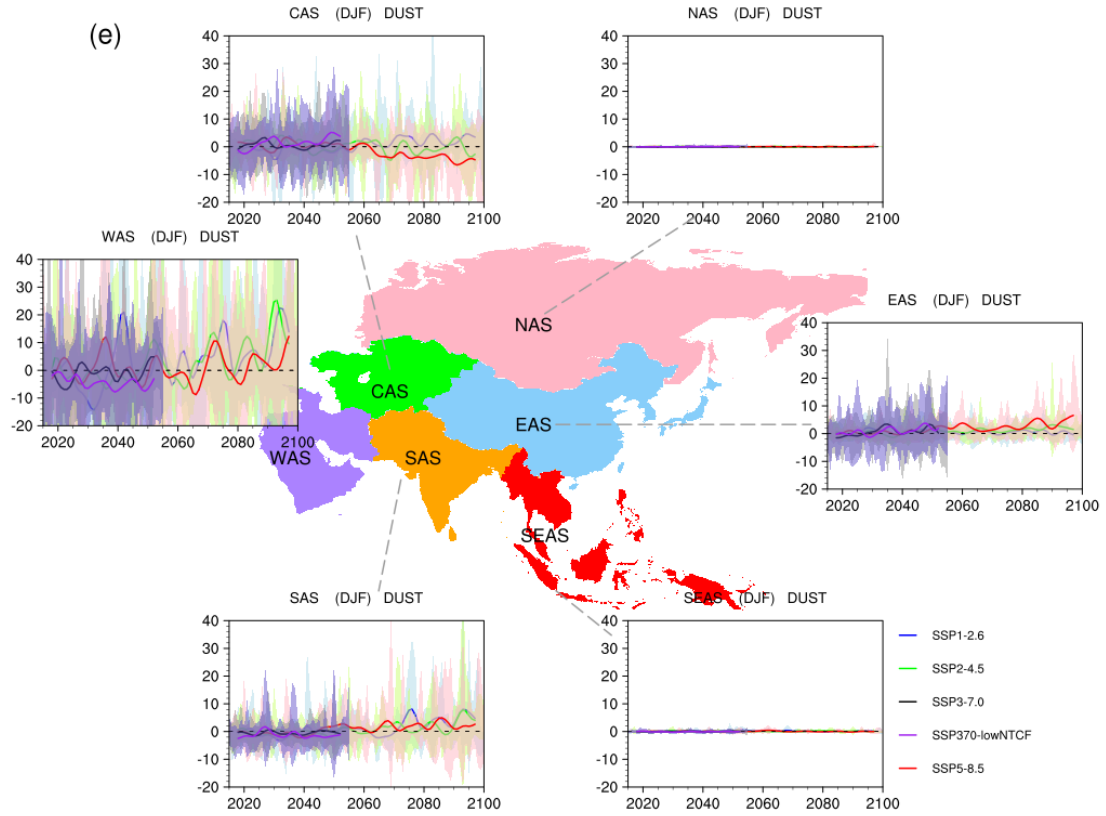
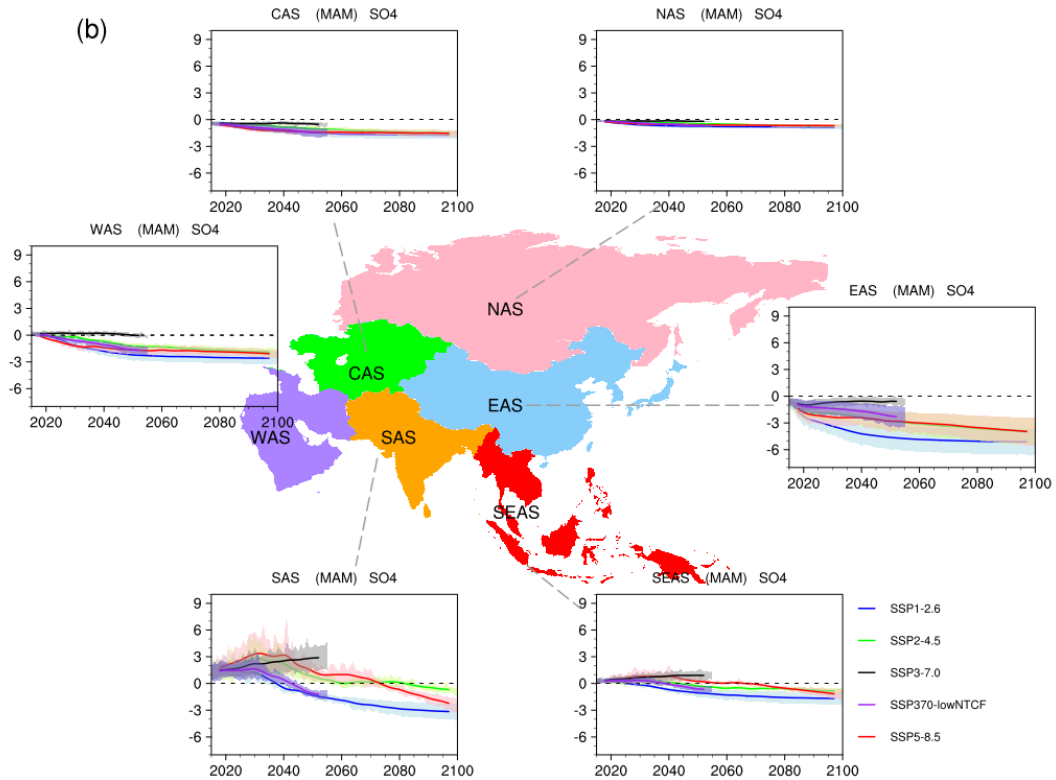
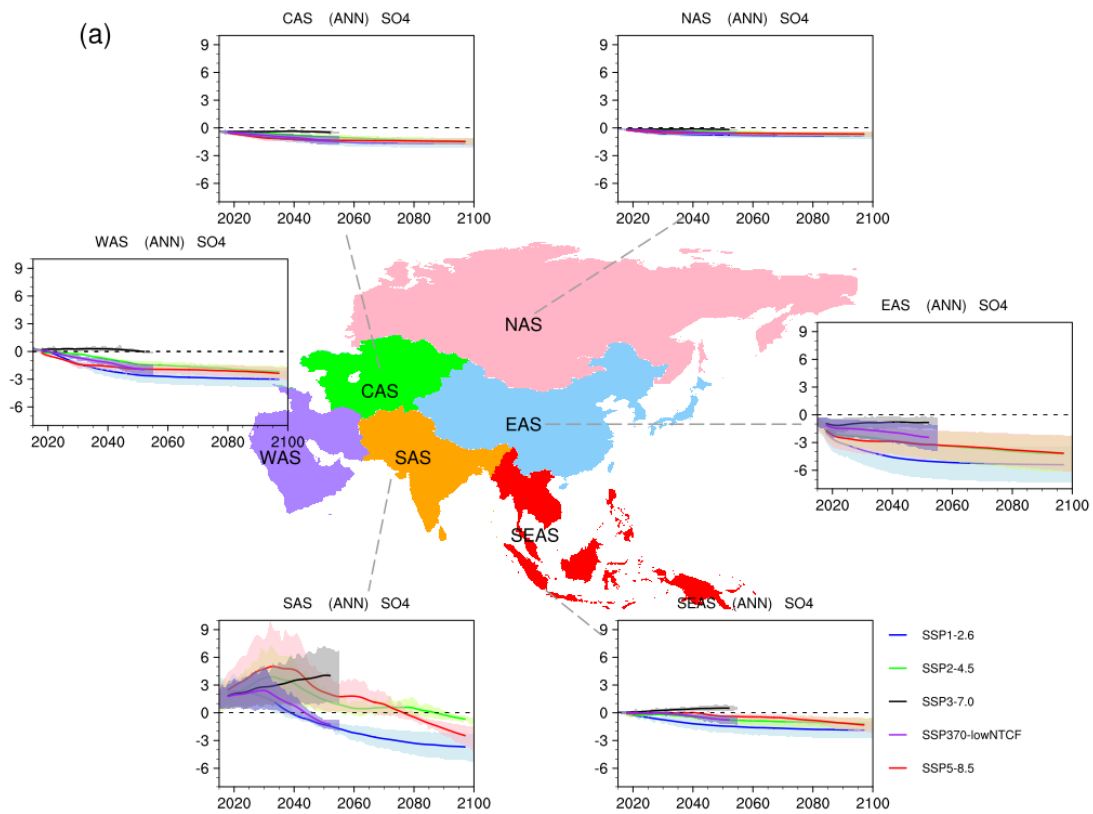
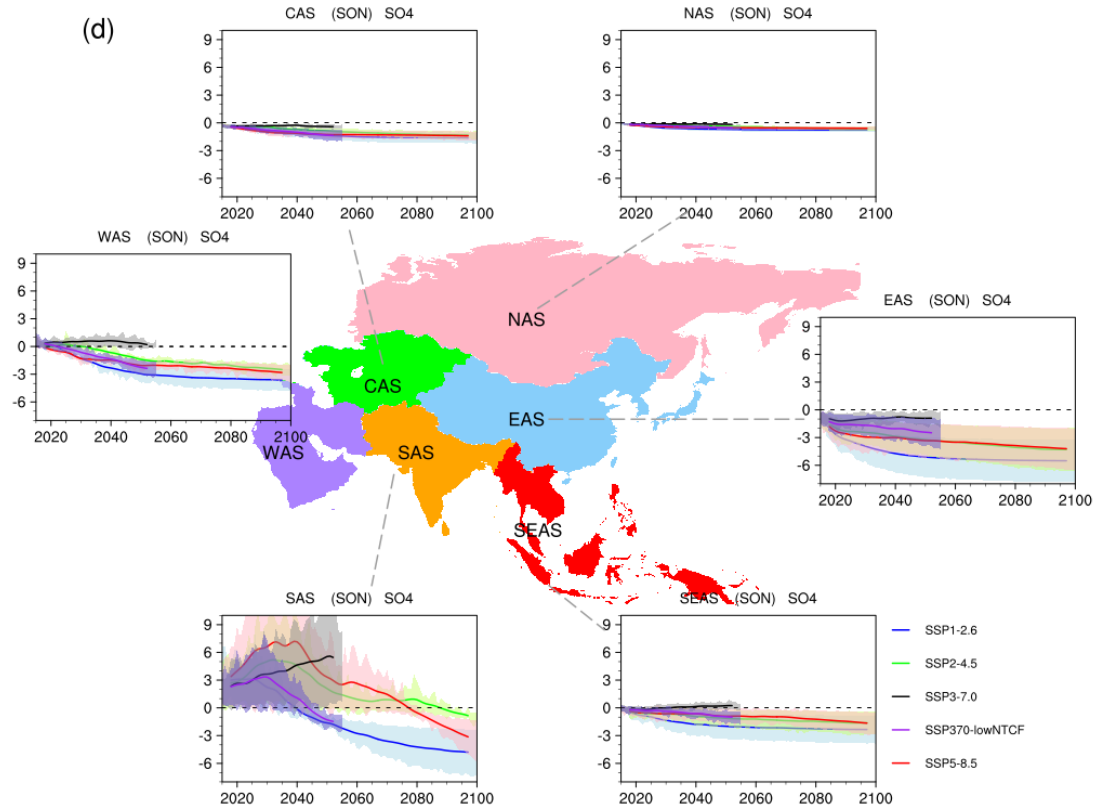
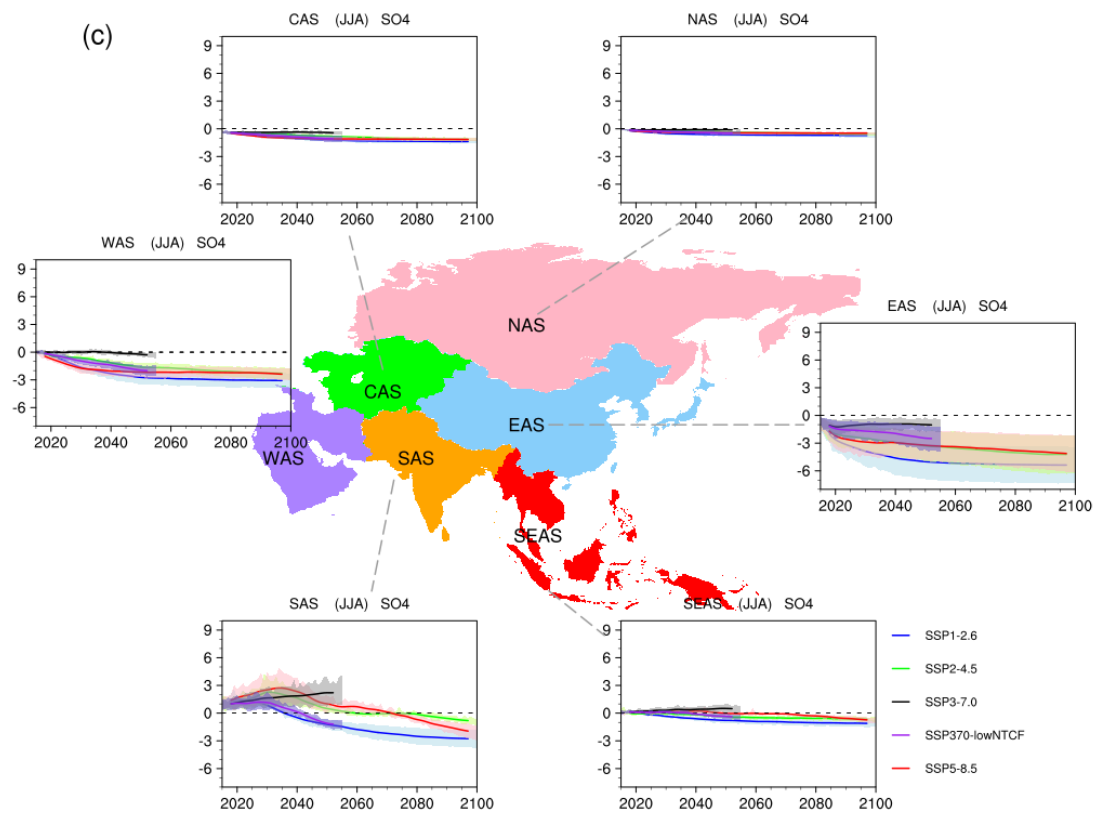


Figure S5 Time evolutions of surface dust concentrations (units: $\mu g/m^3$) in annual (a), spring (b), summer(c), autumn (d) and winter (e) over Asia under SSP1-2.6 (red curves), SSP2-4.5 (green curves), SSP3-7.0 (black curves), SSP370-lowNTCF (purple curves) and SSP5-8.5 (red curves), relative to 1995-2014, where shadings indicate model uncertainty range (1 standard deviation of the simulations).





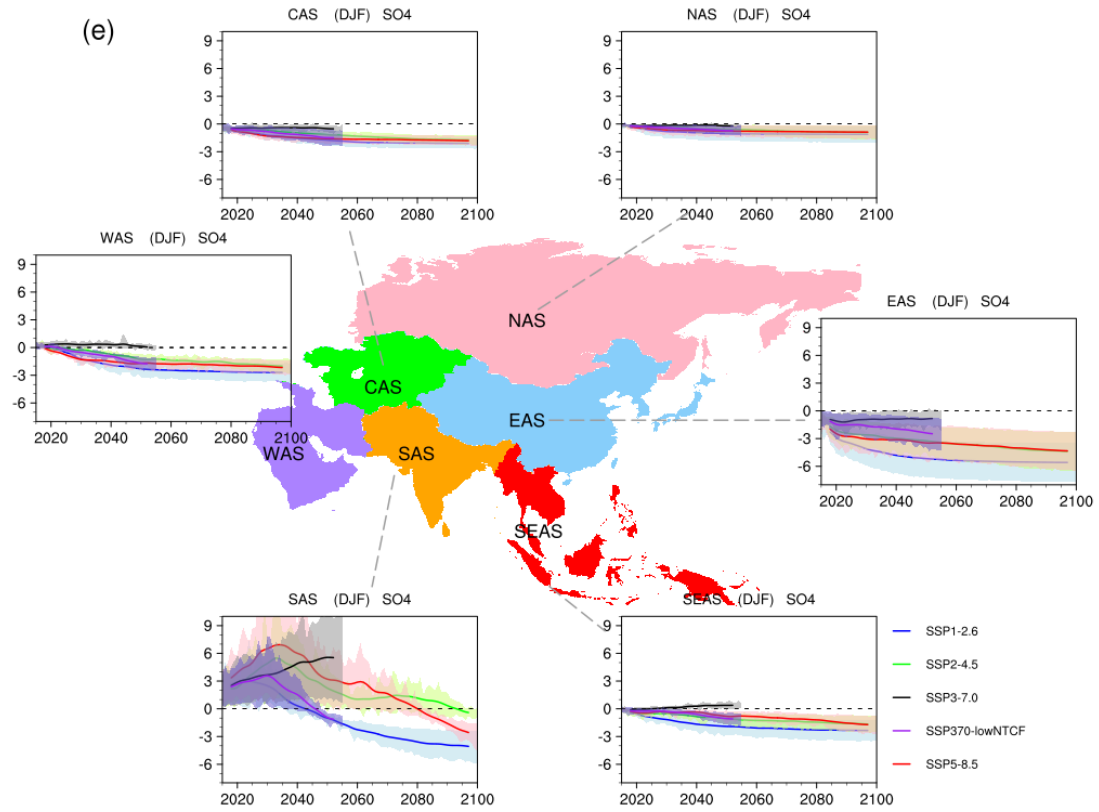
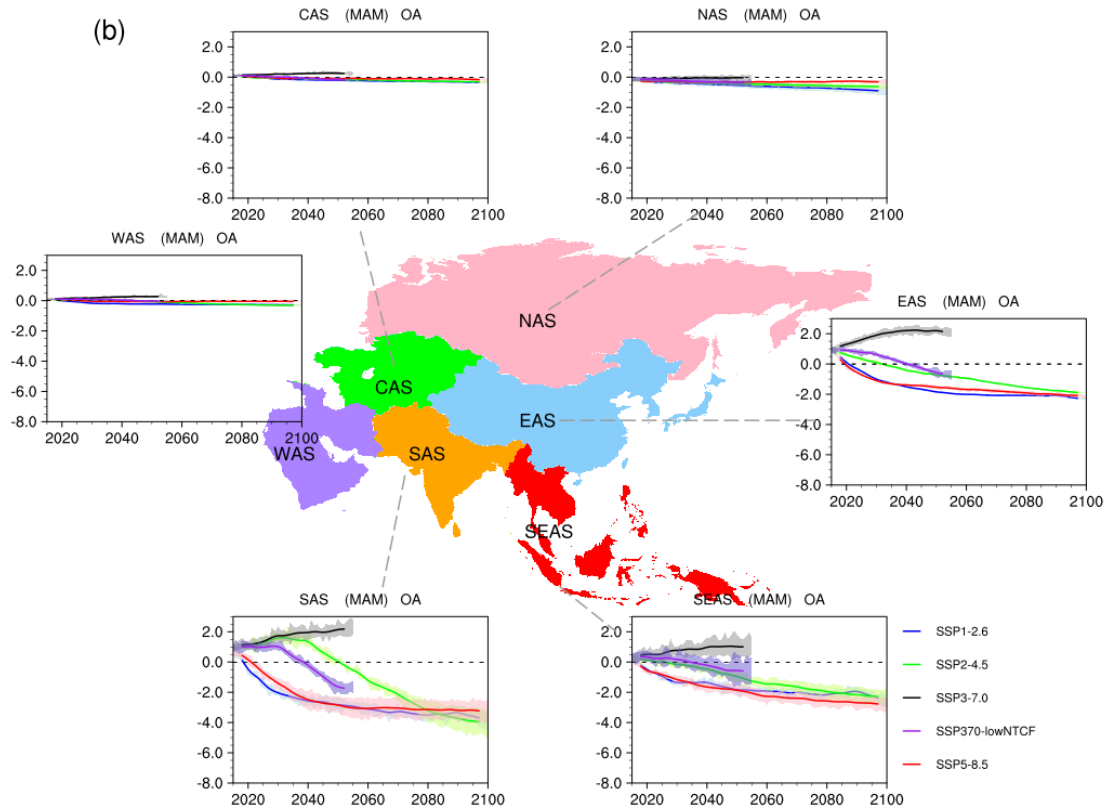
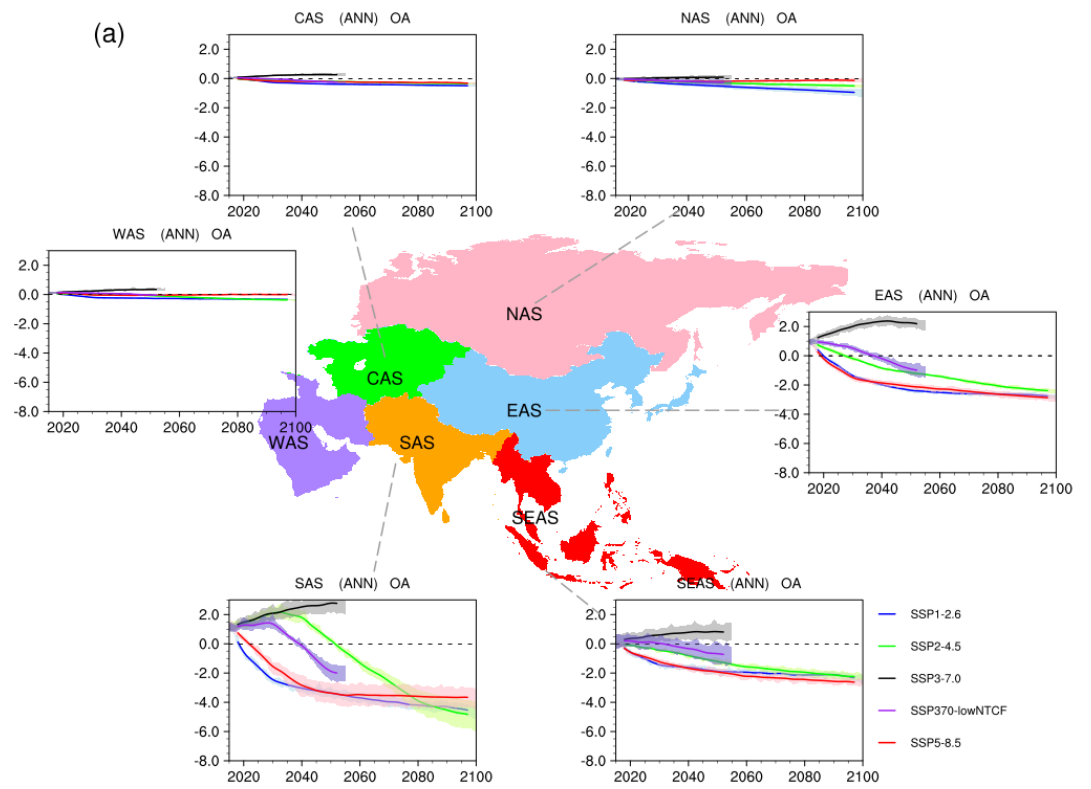
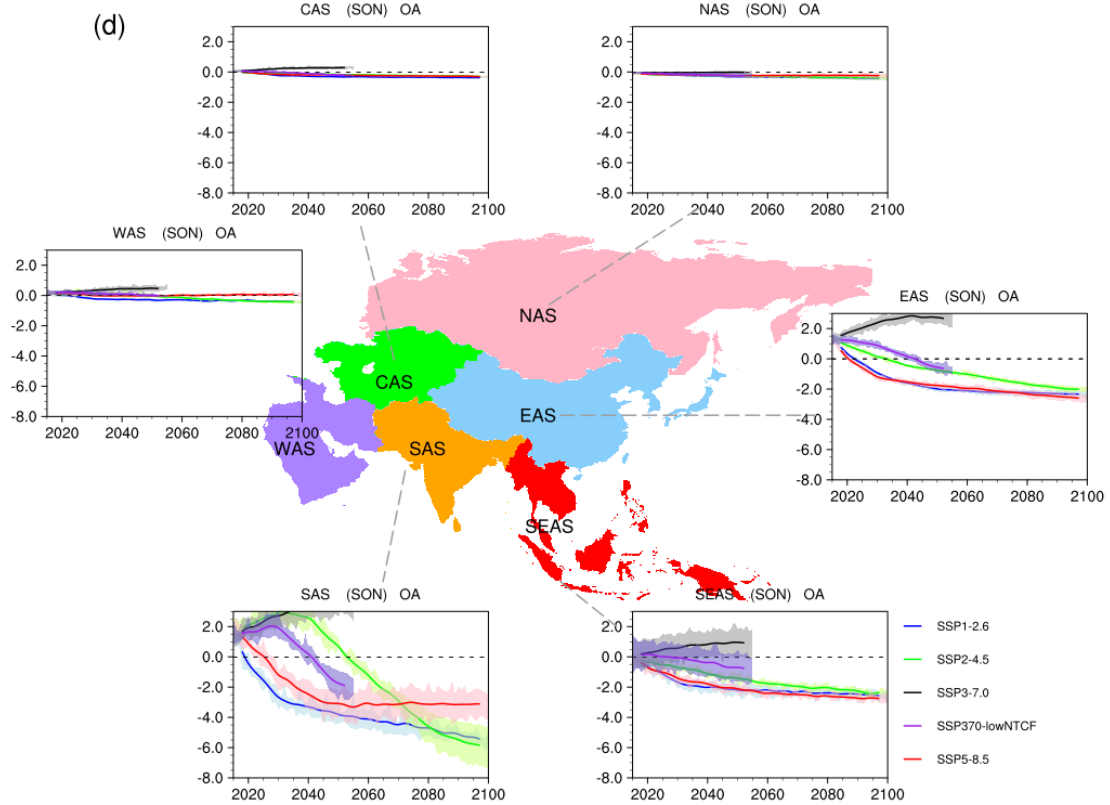
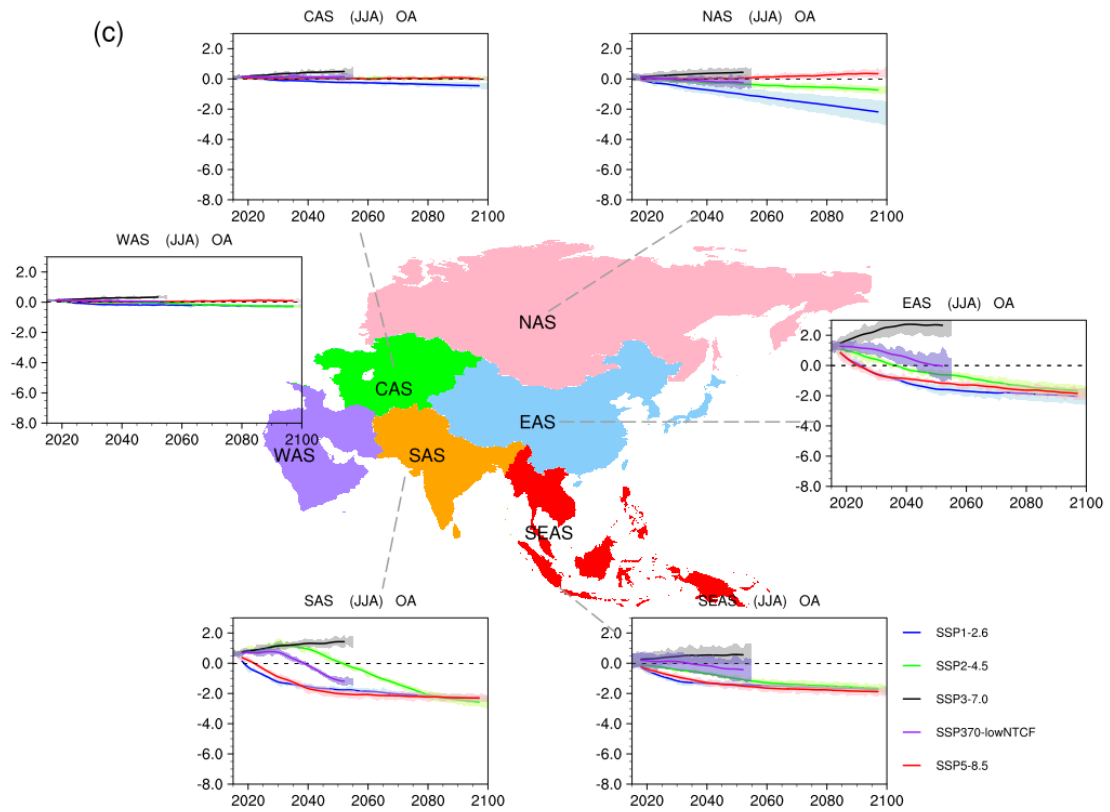


Figure S6 Time evolutions of surface SO₄ concentrations (units: $\mu\text{g}/\text{m}^3$) in annual (a), spring (b), summer (c), autumn (d) and winter (e) over Asia under SSP1-2.6 (red curves), SSP2-4.5 (green curves), SSP3-7.0 (black curves), SSP370-lowNTCF (purple curves) and SSP5-8.5 (red curves), relative to 1995-2014, where shadings indicate model uncertainty range (1 standard deviation of the simulations).





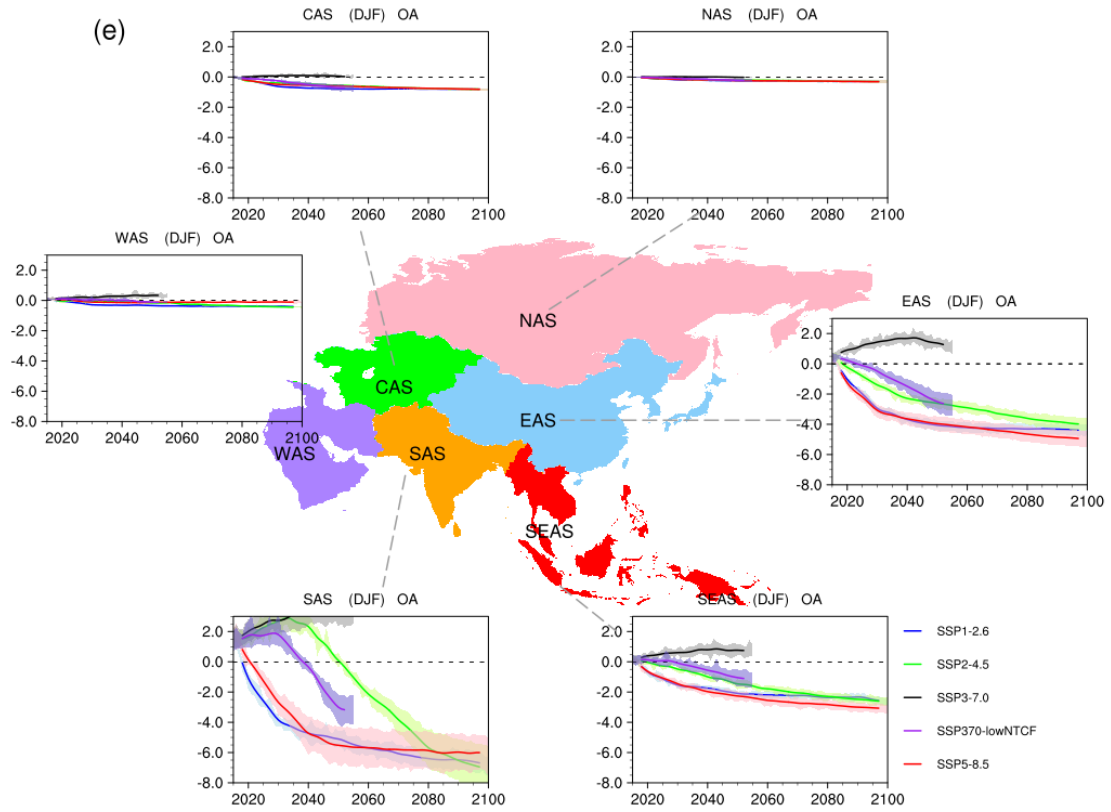
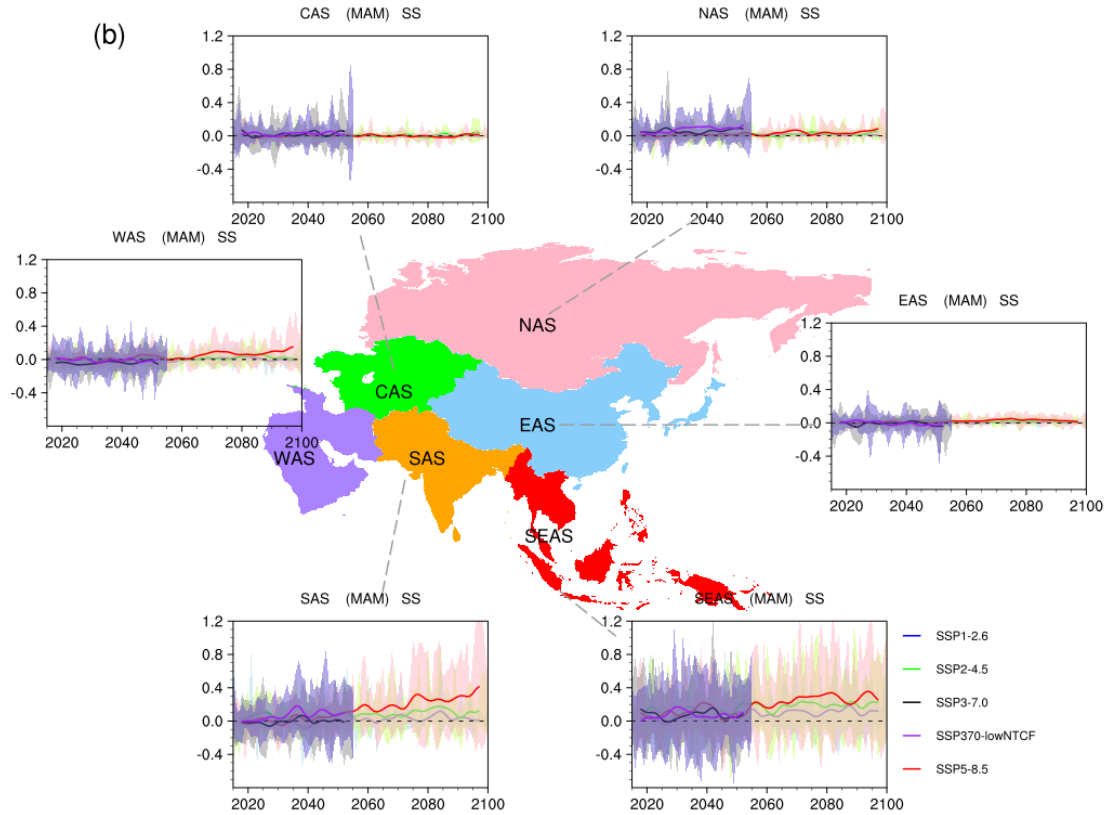
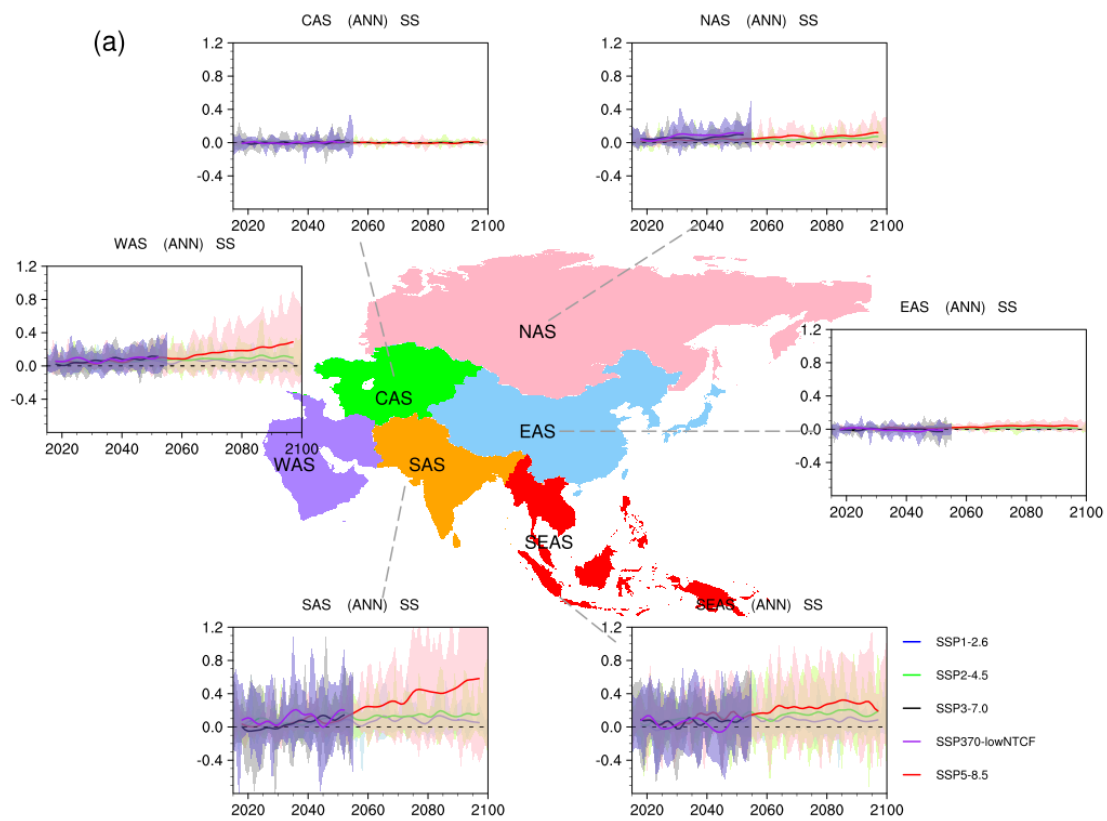
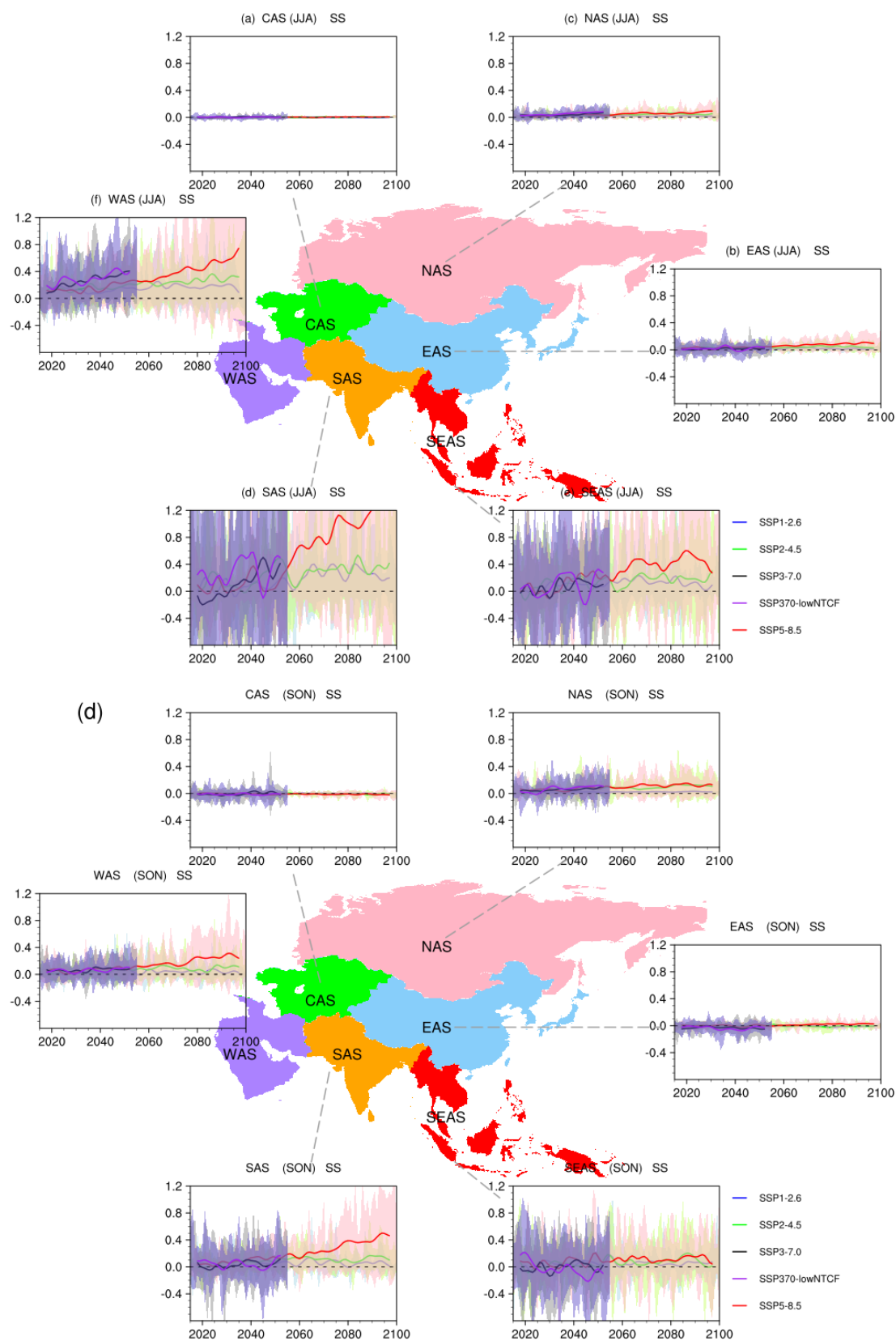


Figure S7 Time evolutions of surface organic aerosol (OA) concentrations (units: $\mu\text{g}/\text{m}^3$) in annual (a), spring (b), summer(c), autumn (d) and winter (e) over Asia under SSP1-2.6 (red curves), SSP2-4.5 (green curves), SSP3-7.0 (black curves), SSP370-lowNTCF (purple curves) and SSP5-8.5 (red curves), relative to 1995-2014, where shadings indicate model uncertainty range (1 standard deviation of the simulations).





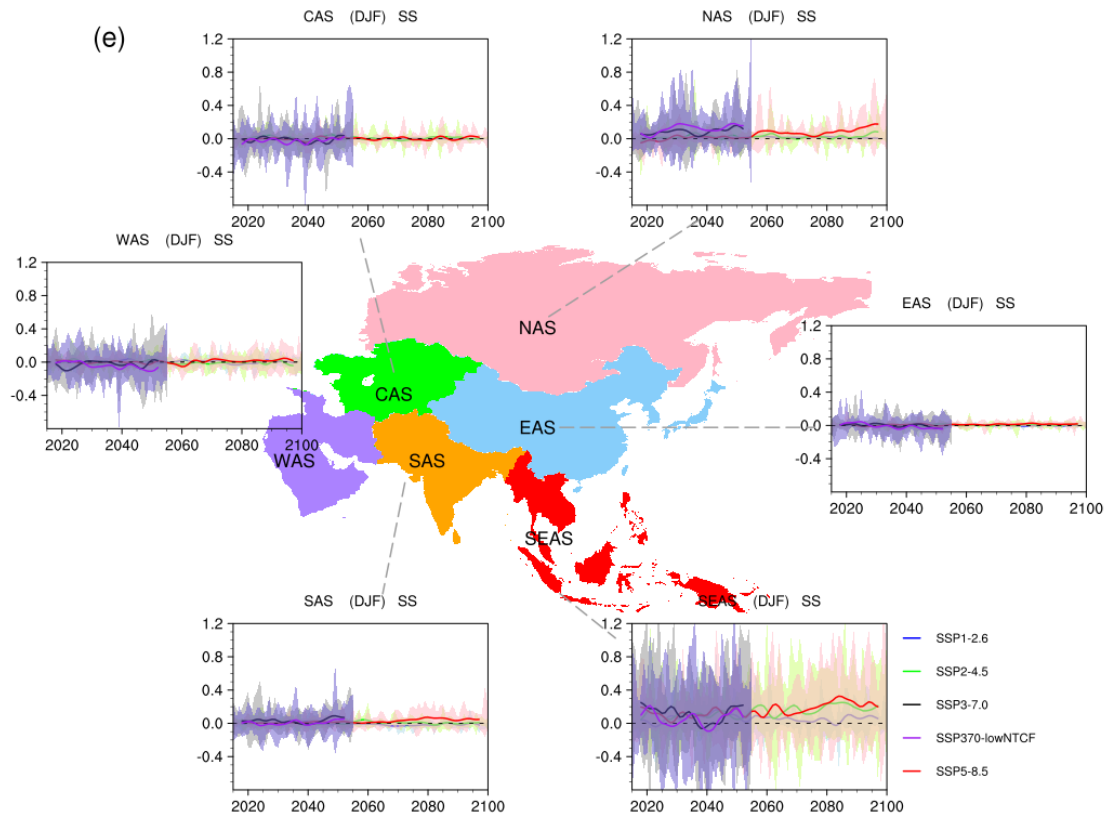
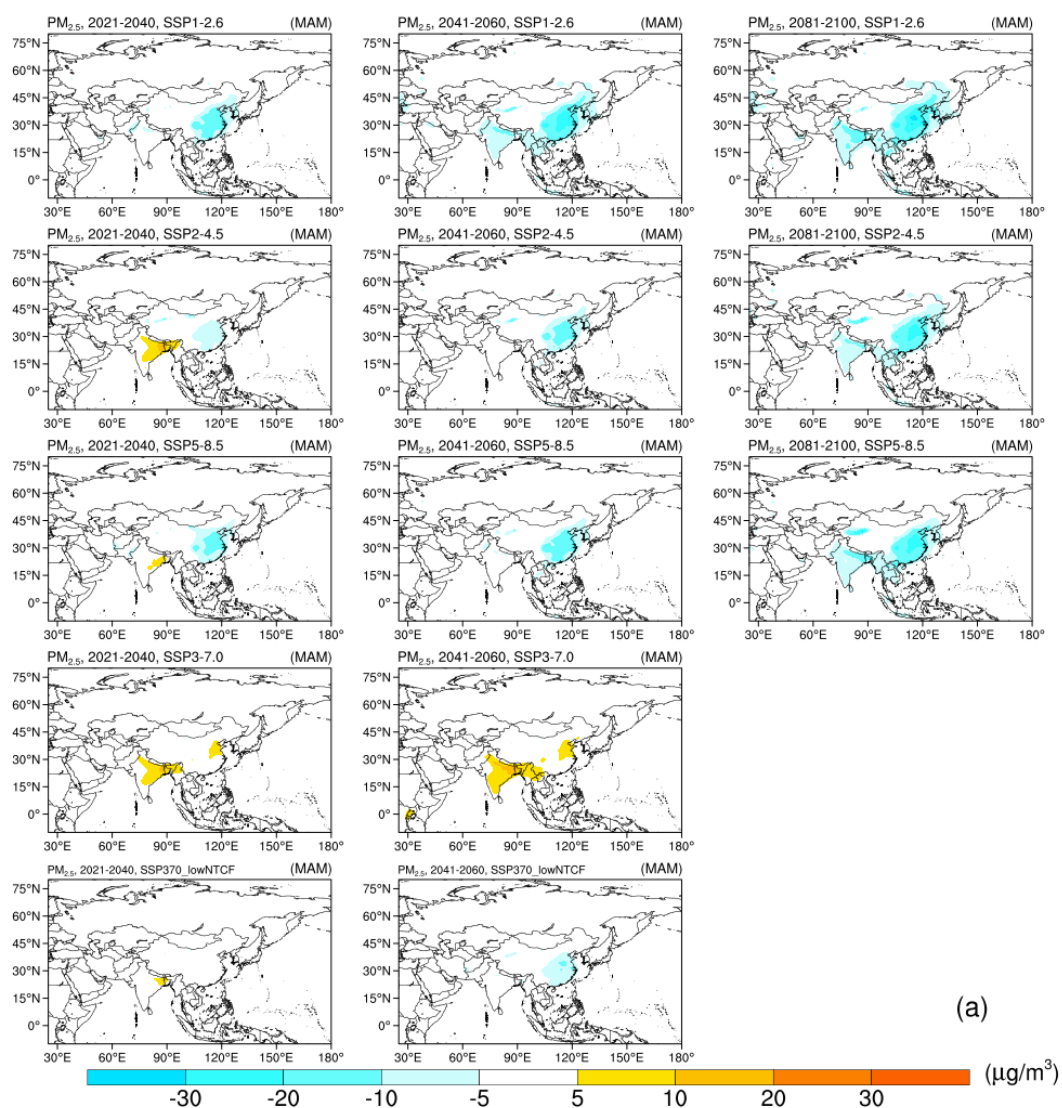
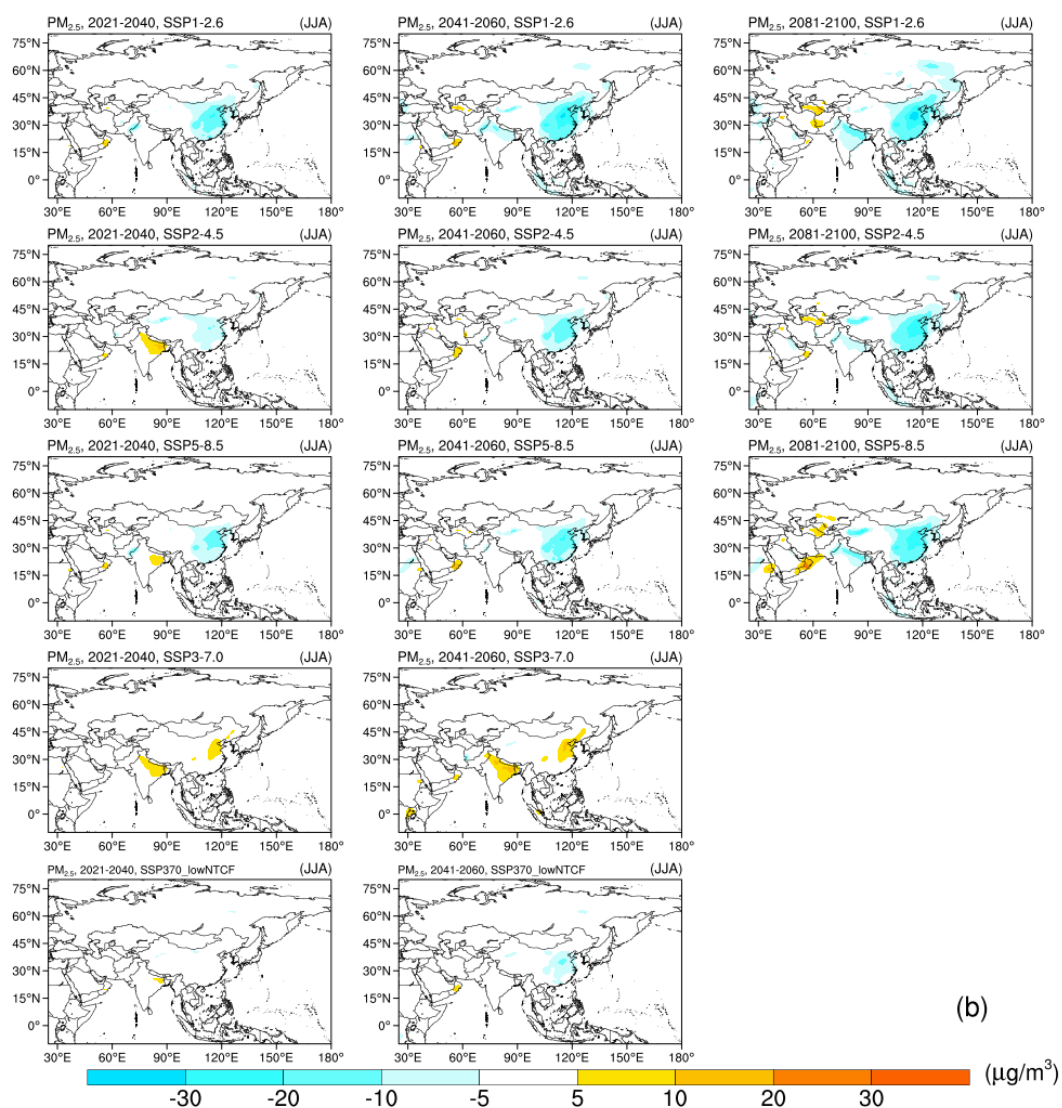
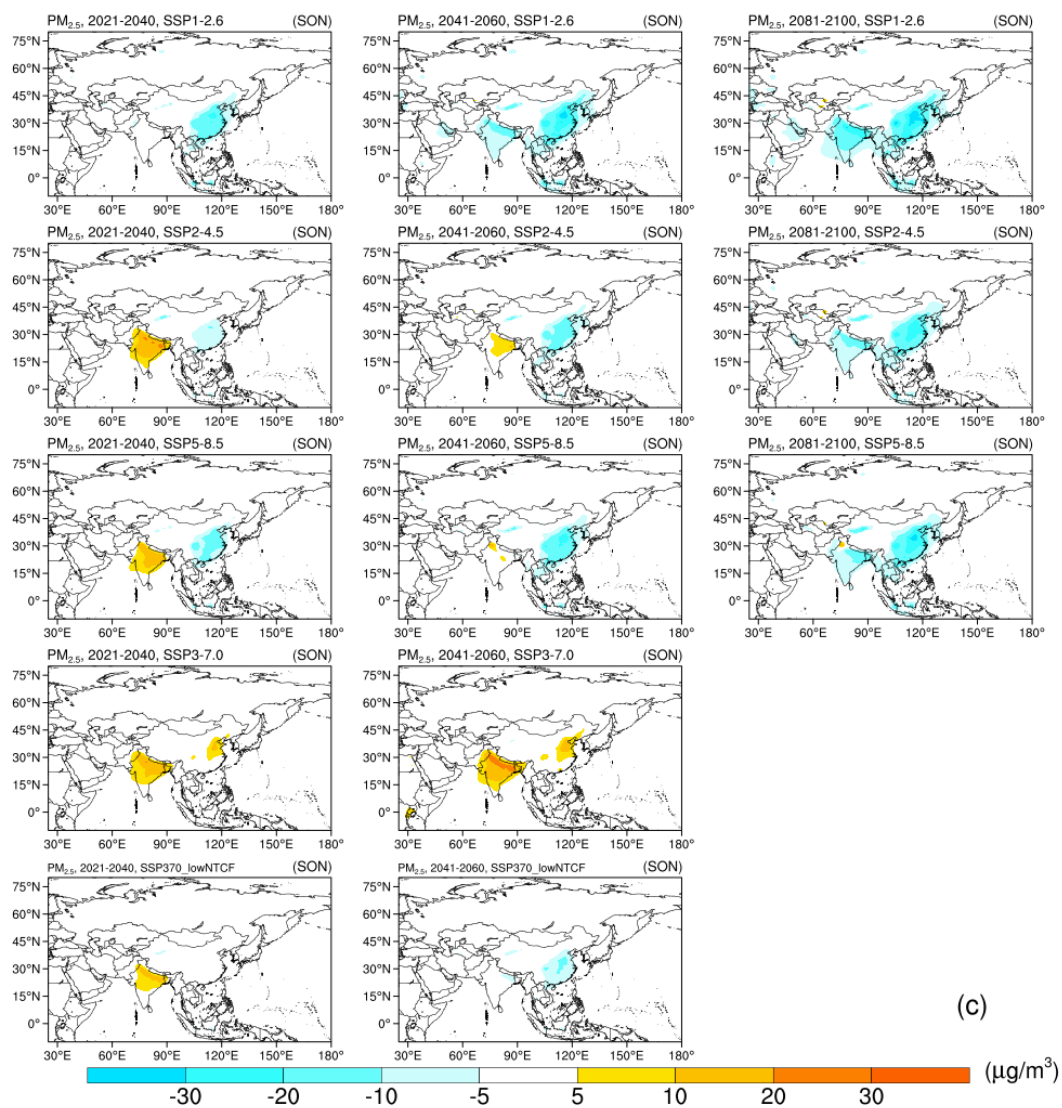


Figure S8 Time evolutions of surface sea salt (SS) concentrations (units: $\mu\text{g}/\text{m}^3$) in annual (a), spring (b), summer (c), autumn (d) and winter (e) over Asia under SSP1-2.6 (red curves), SSP2-4.5 (green curves), SSP3-7.0 (black curves), SSP370-lowNTCF (purple curves) and SSP5-8.5 (red curves), relative to 1995-2014, where shadings indicate model uncertainty range (1 standard deviation of the simulations).



(a)





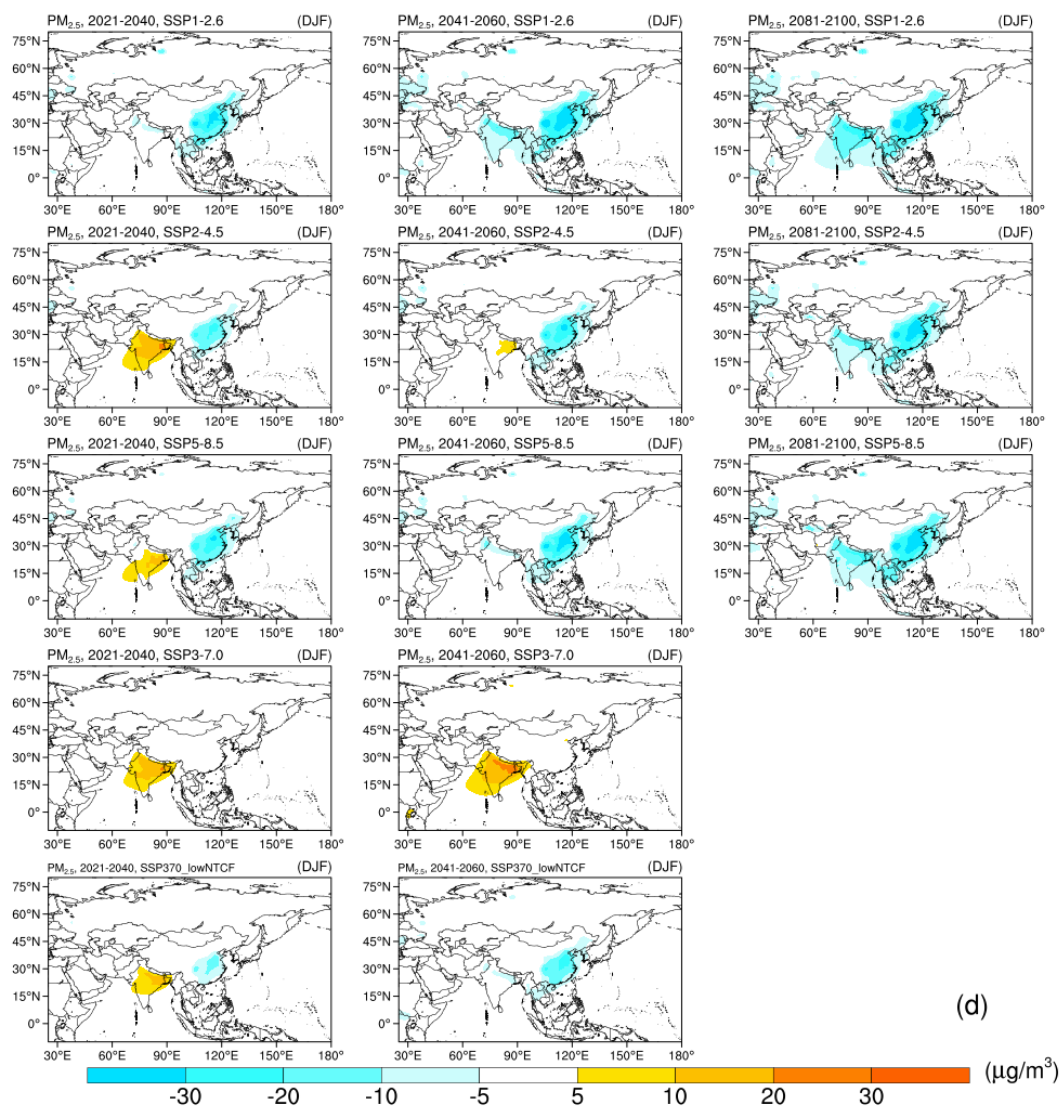
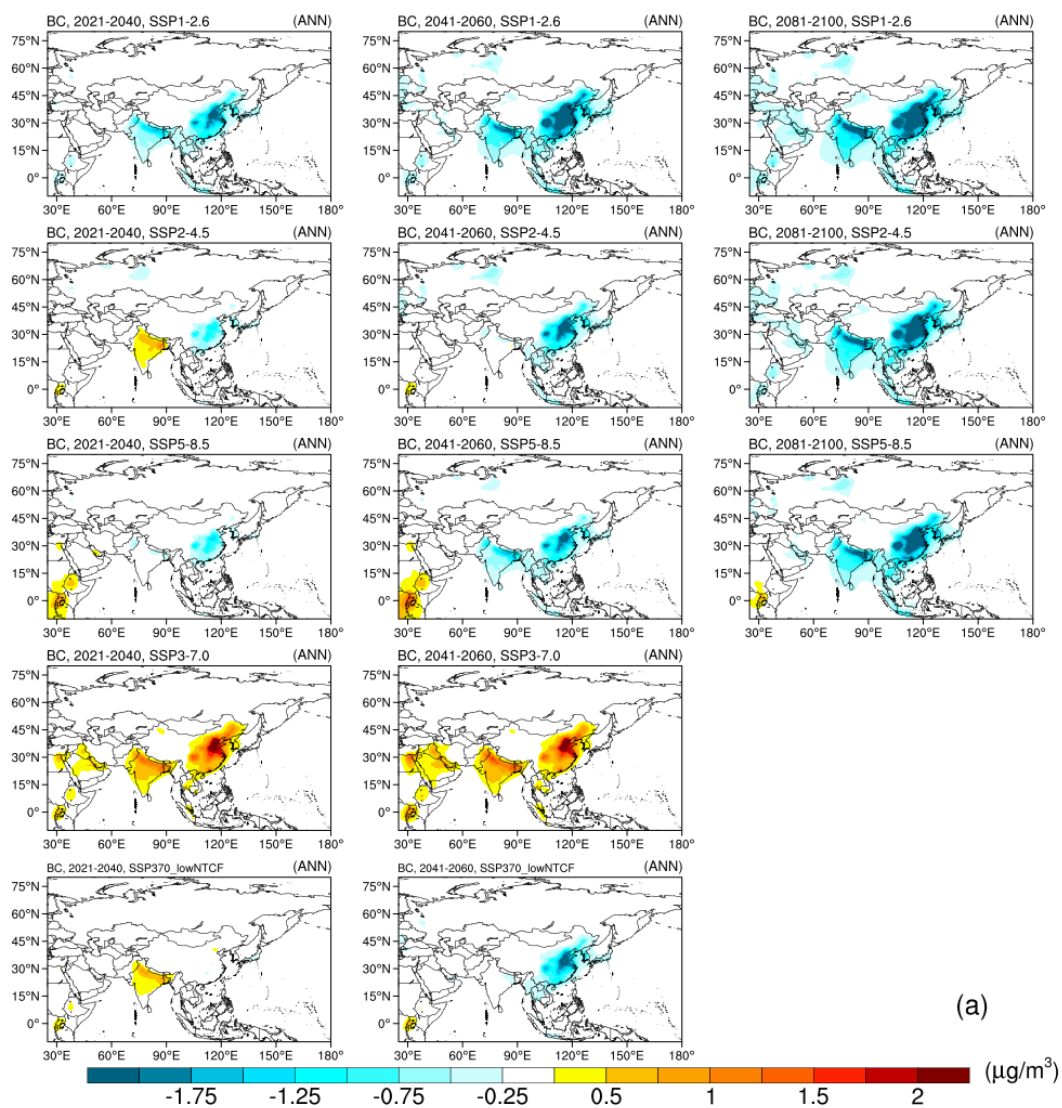
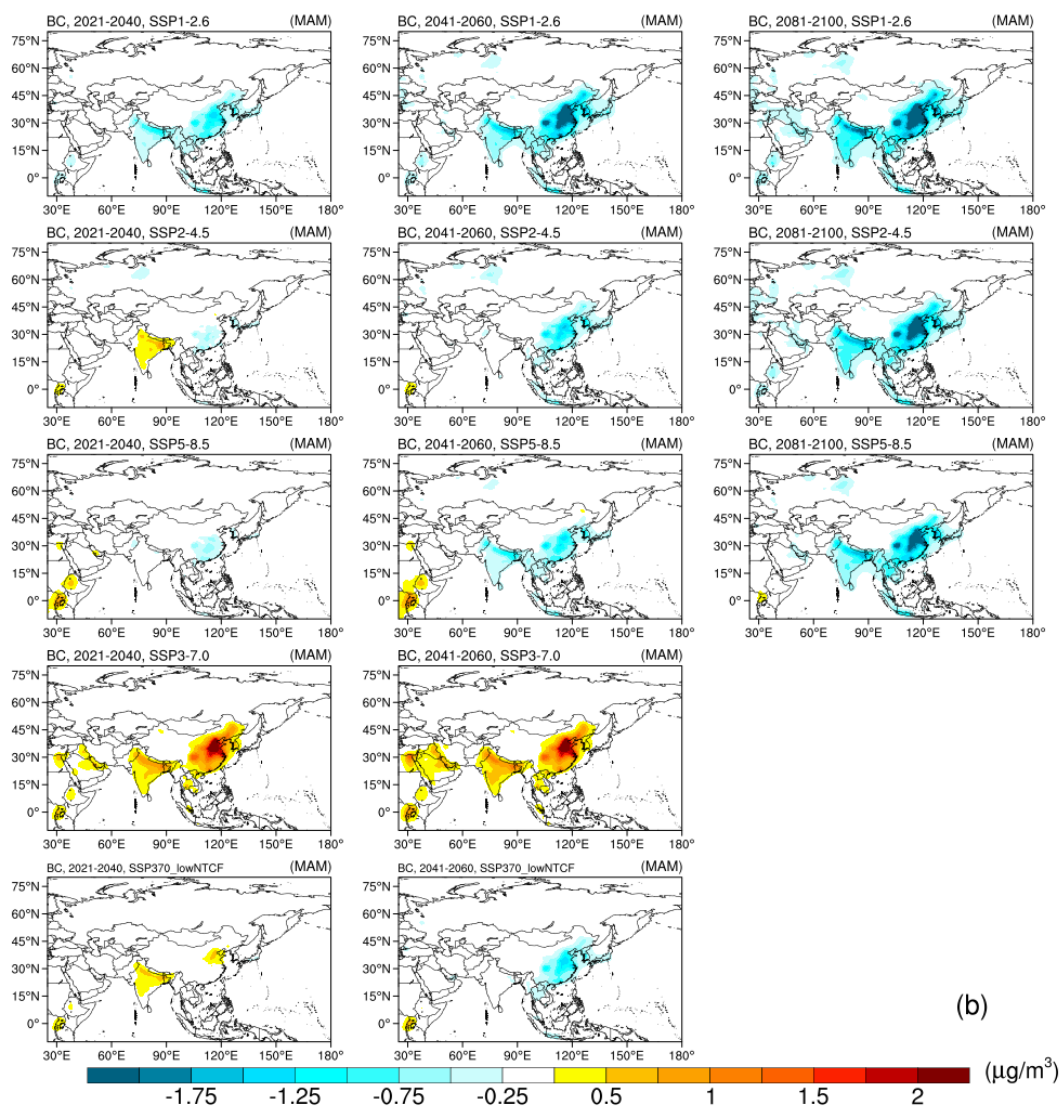
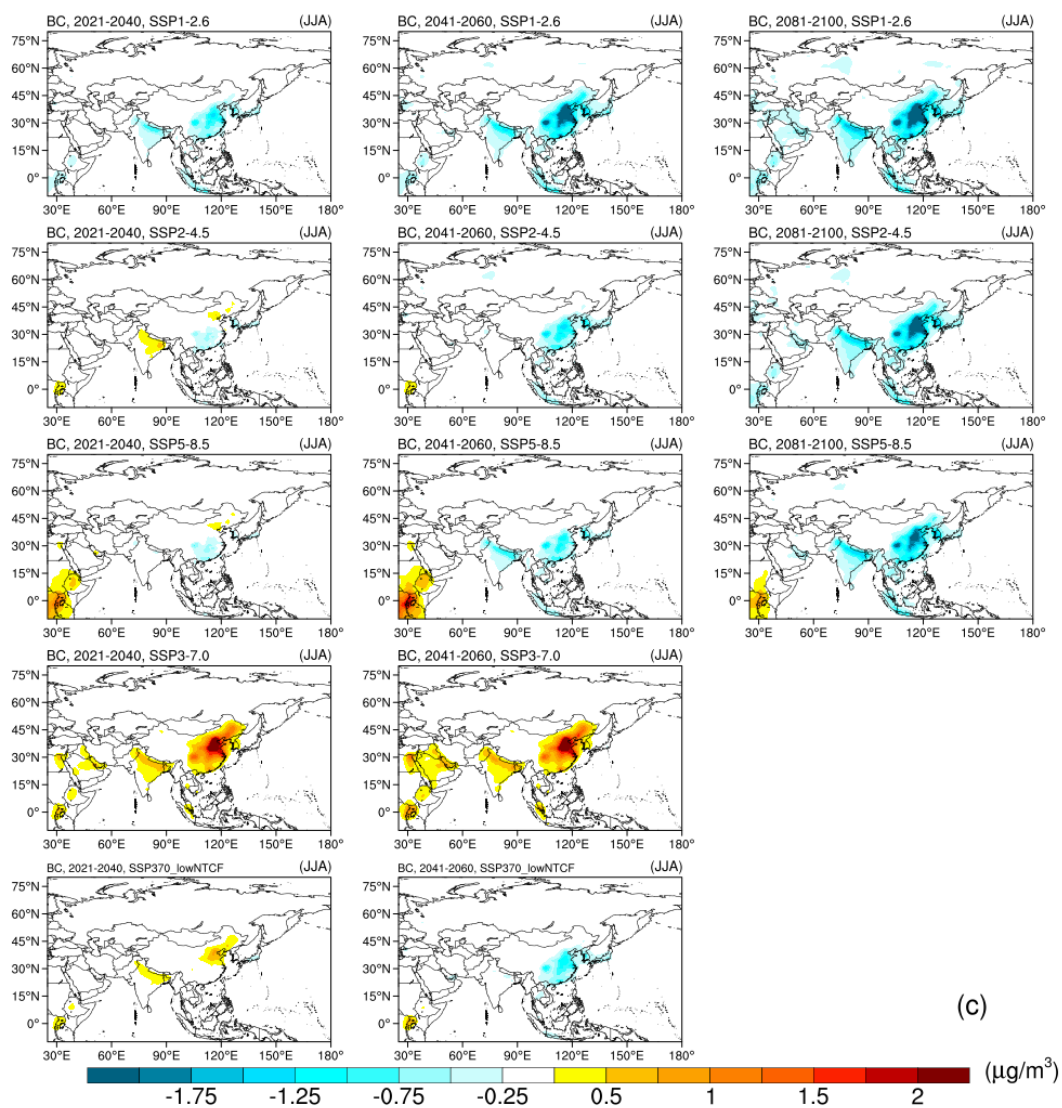


Figure S9 Spatial distribution of projected changes in surface $PM_{2.5}$ concentrations in spring (a), summer (b), autumn (c) and winter (d) (units: $\mu g/m^3$) during 2021–2040, 2041–2060 and 2081–2100 under SSPs, relative to 1995–2014.

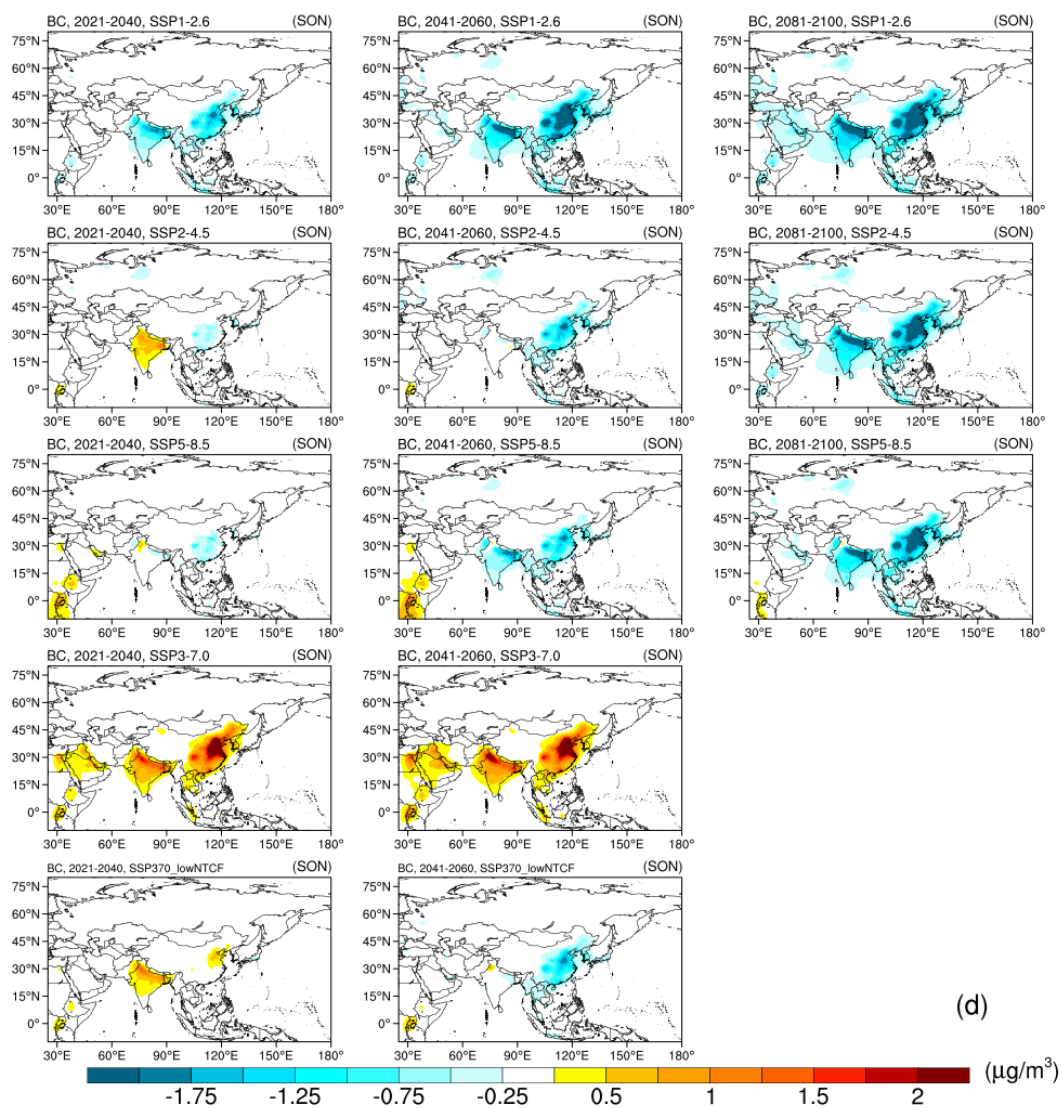


(a)





(c)



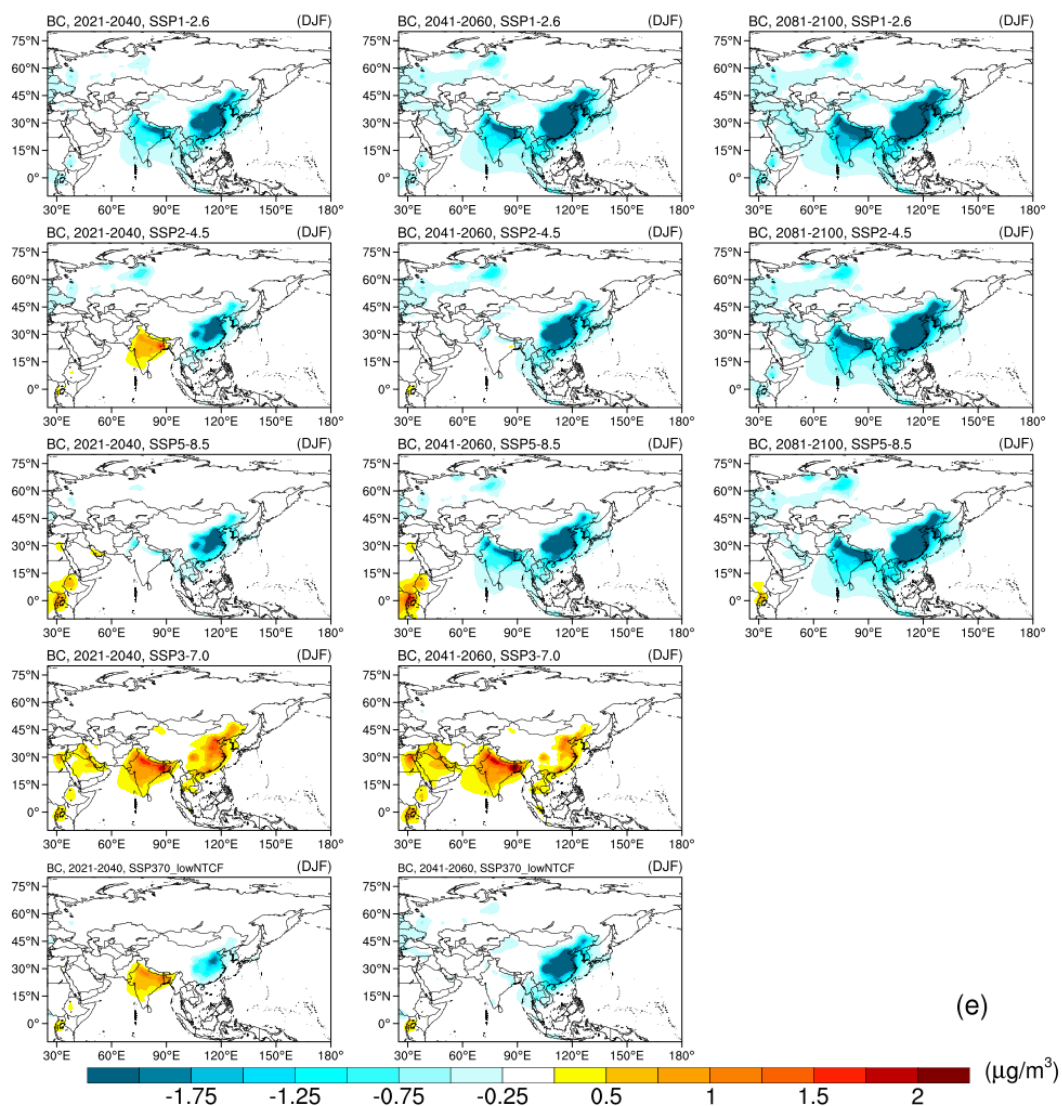
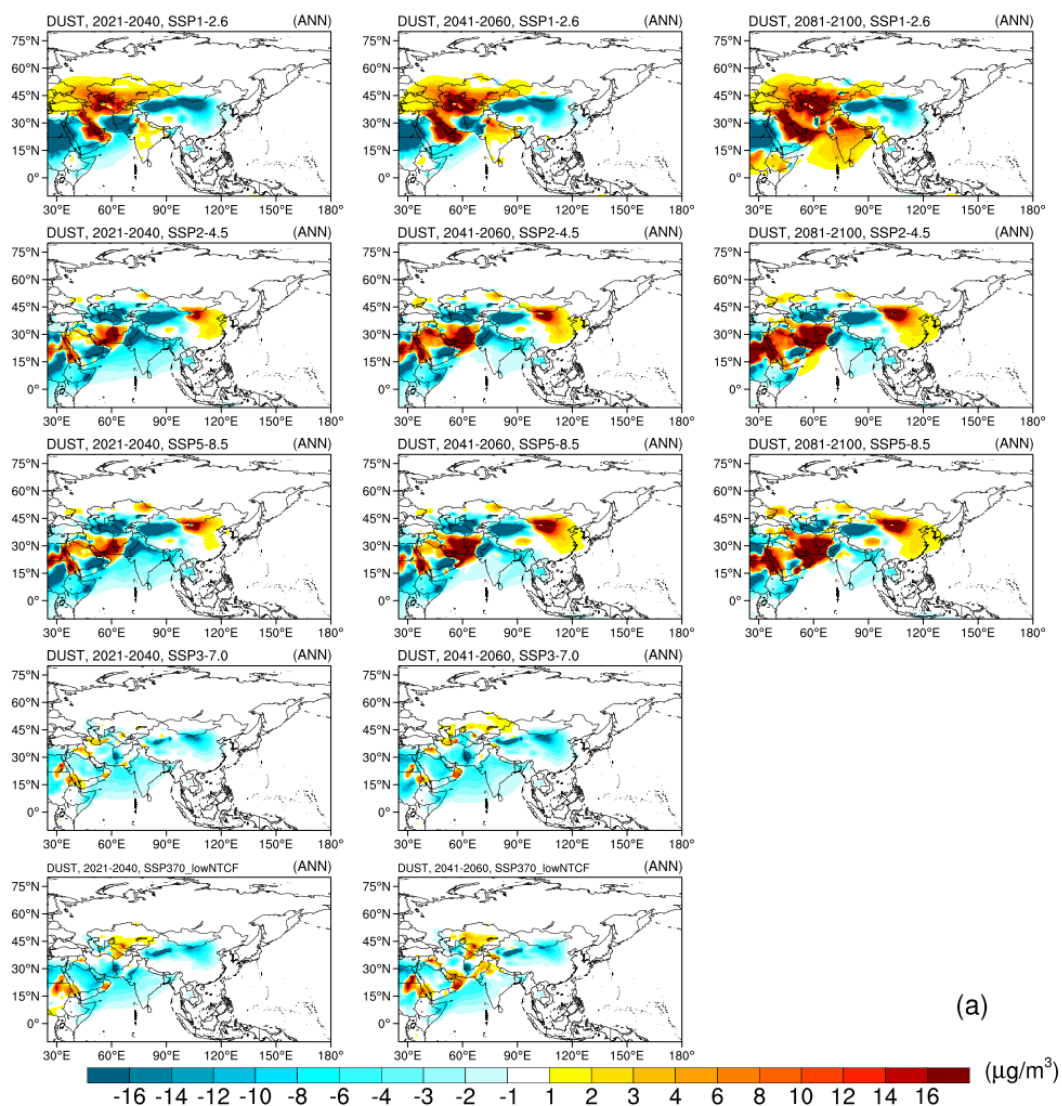
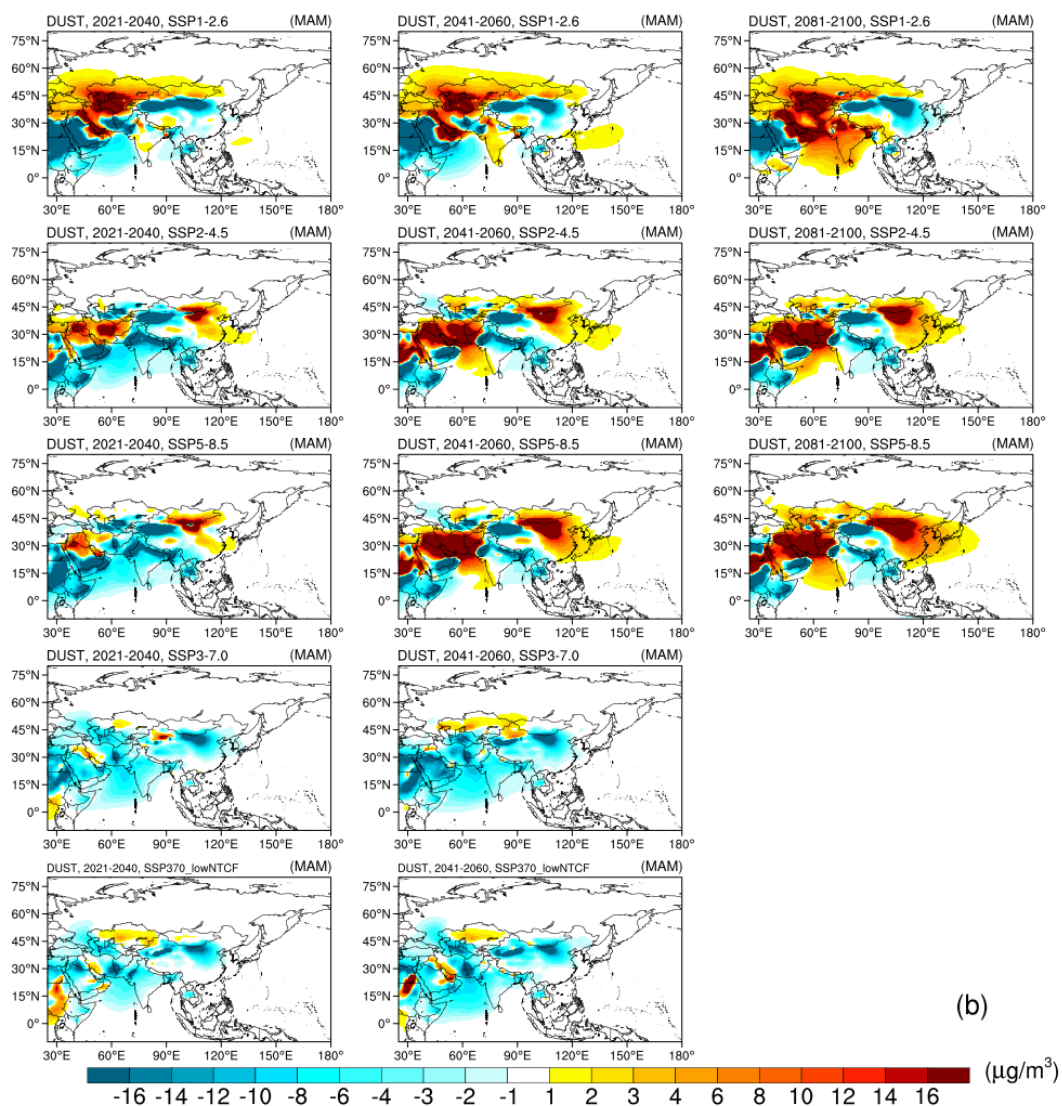
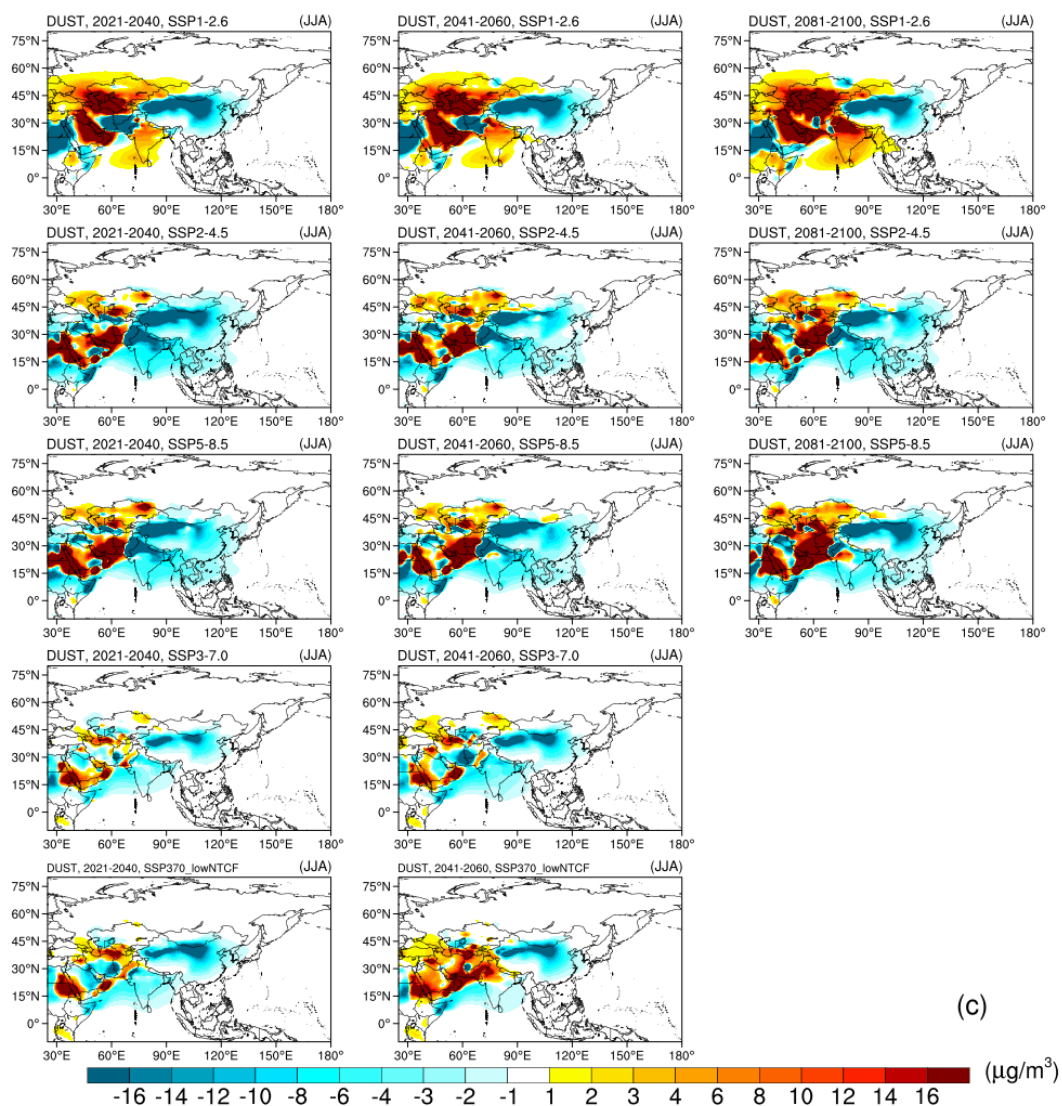


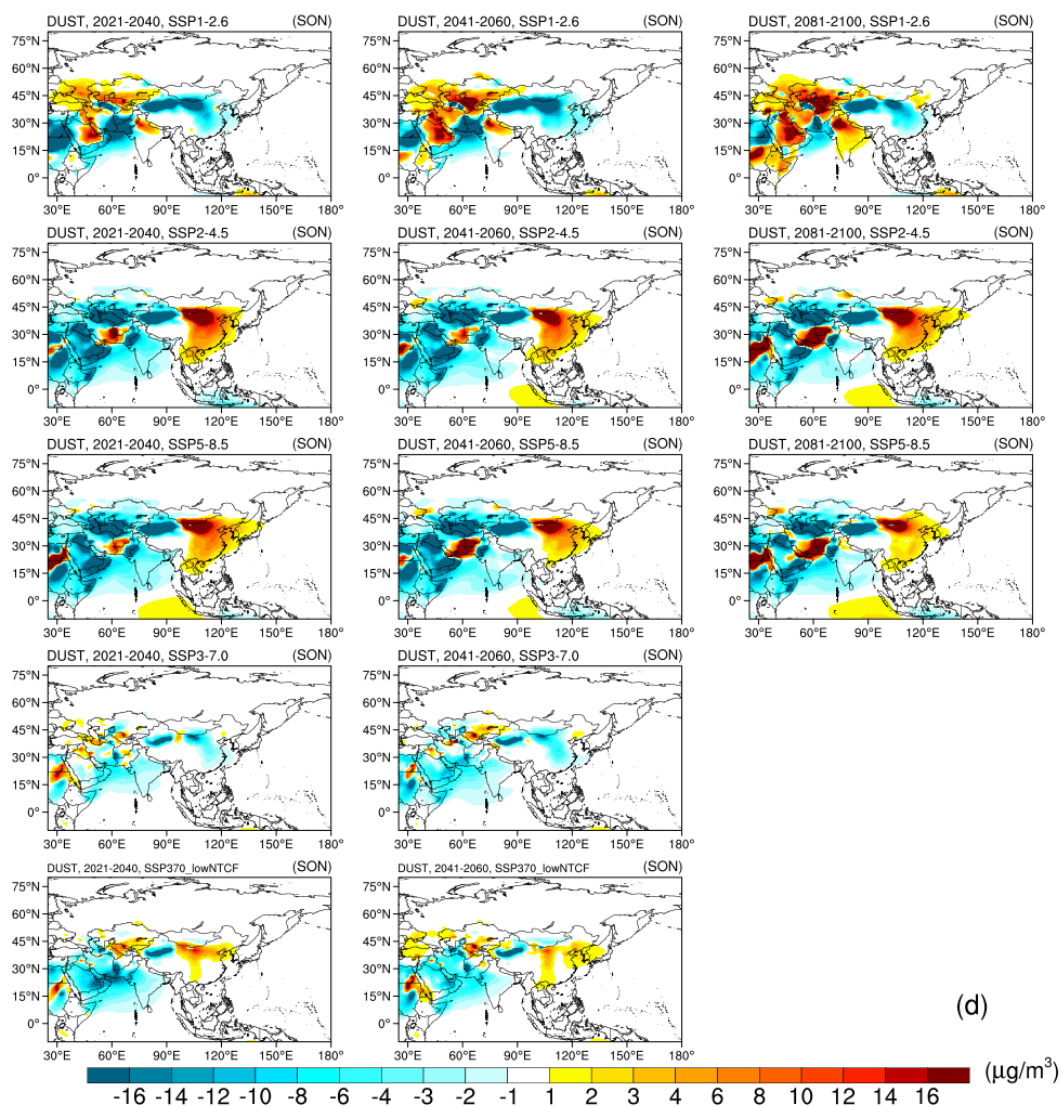
Figure S10 Spatial distribution of projected changes in surface BC concentrations in annual (a), spring (b), summer (c), autumn (d) and winter (e) (units: $\mu\text{g}/\text{m}^3$) during 2021–2040, 2041–2060 and 2081–2100 under SSPs, relative to 1995–2014.







(c)



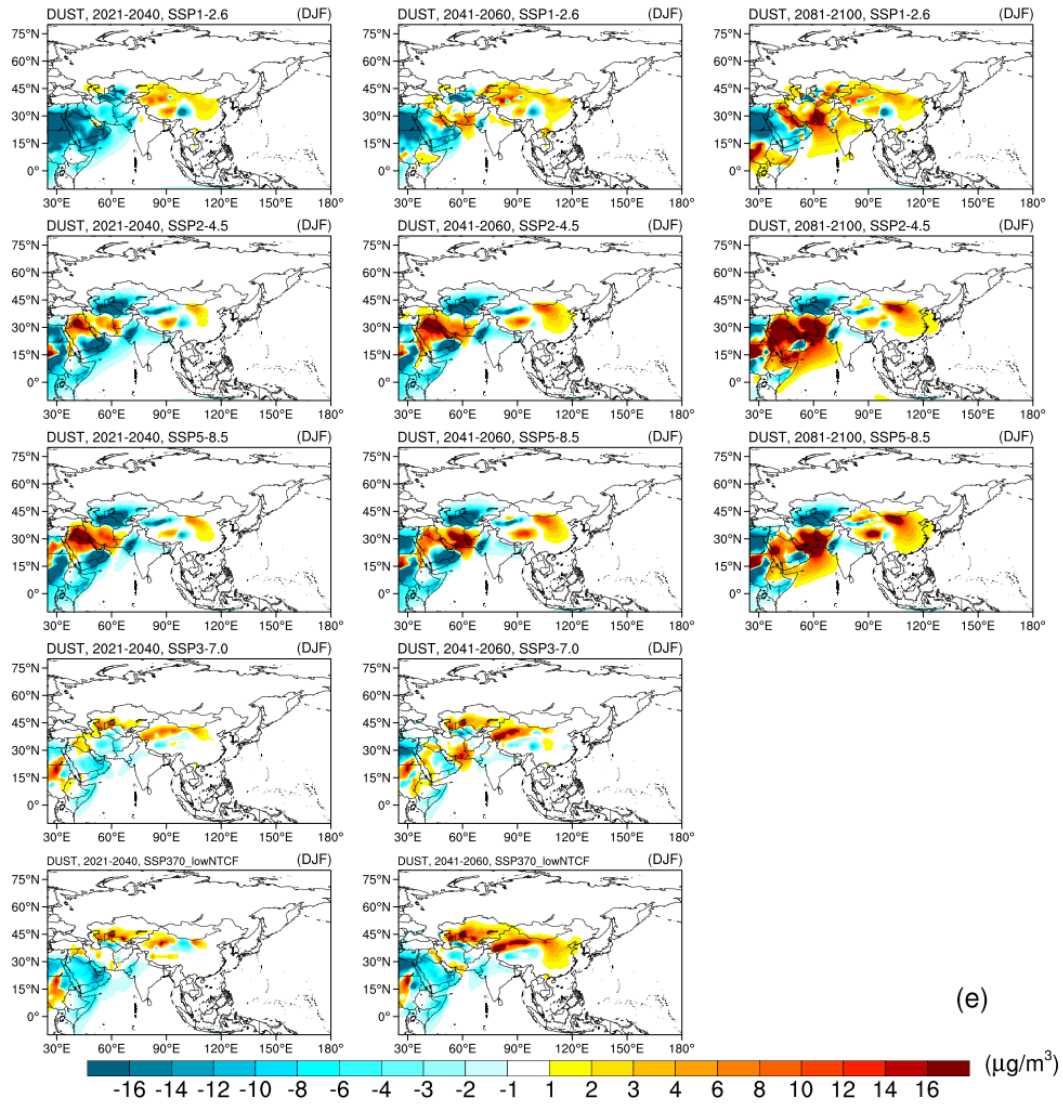
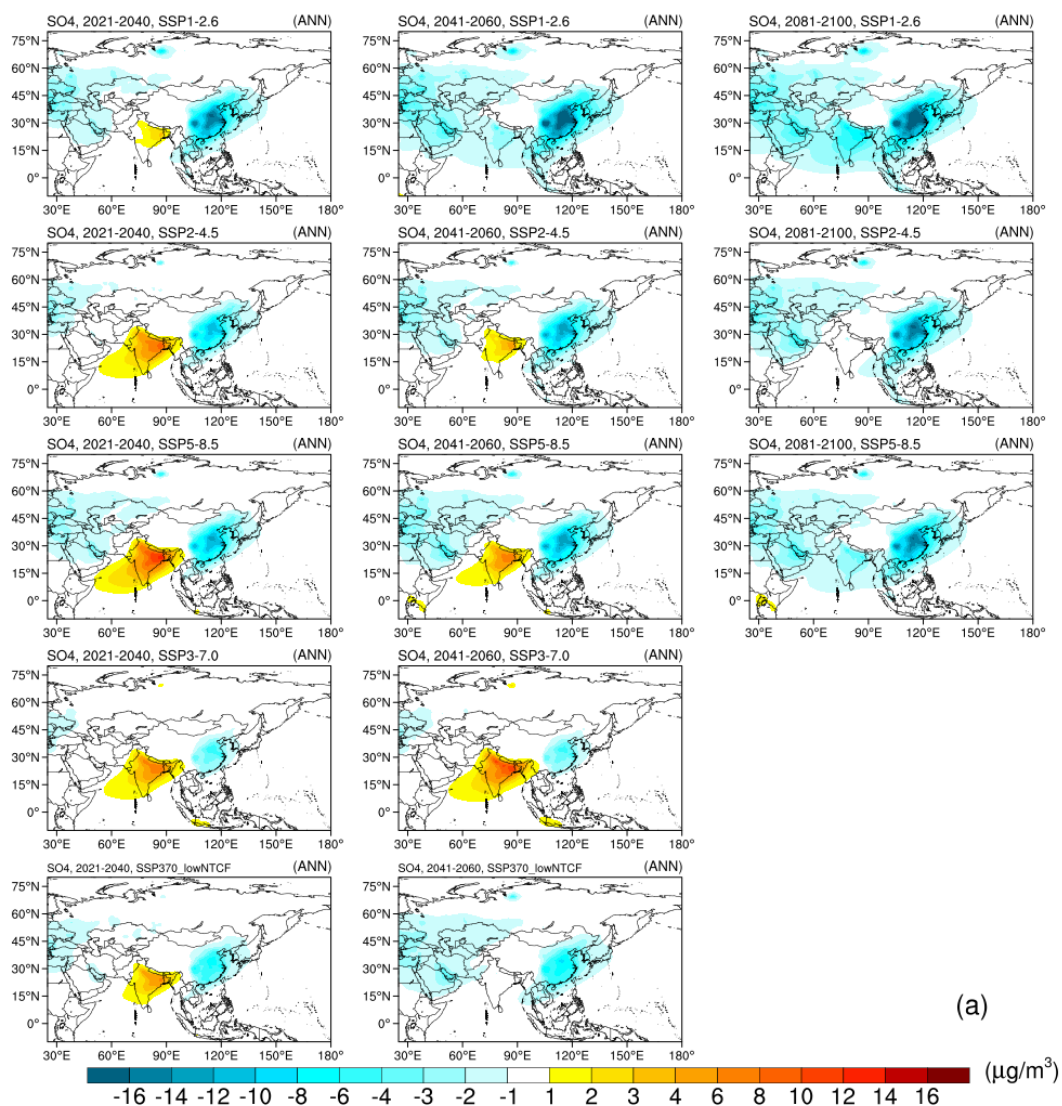
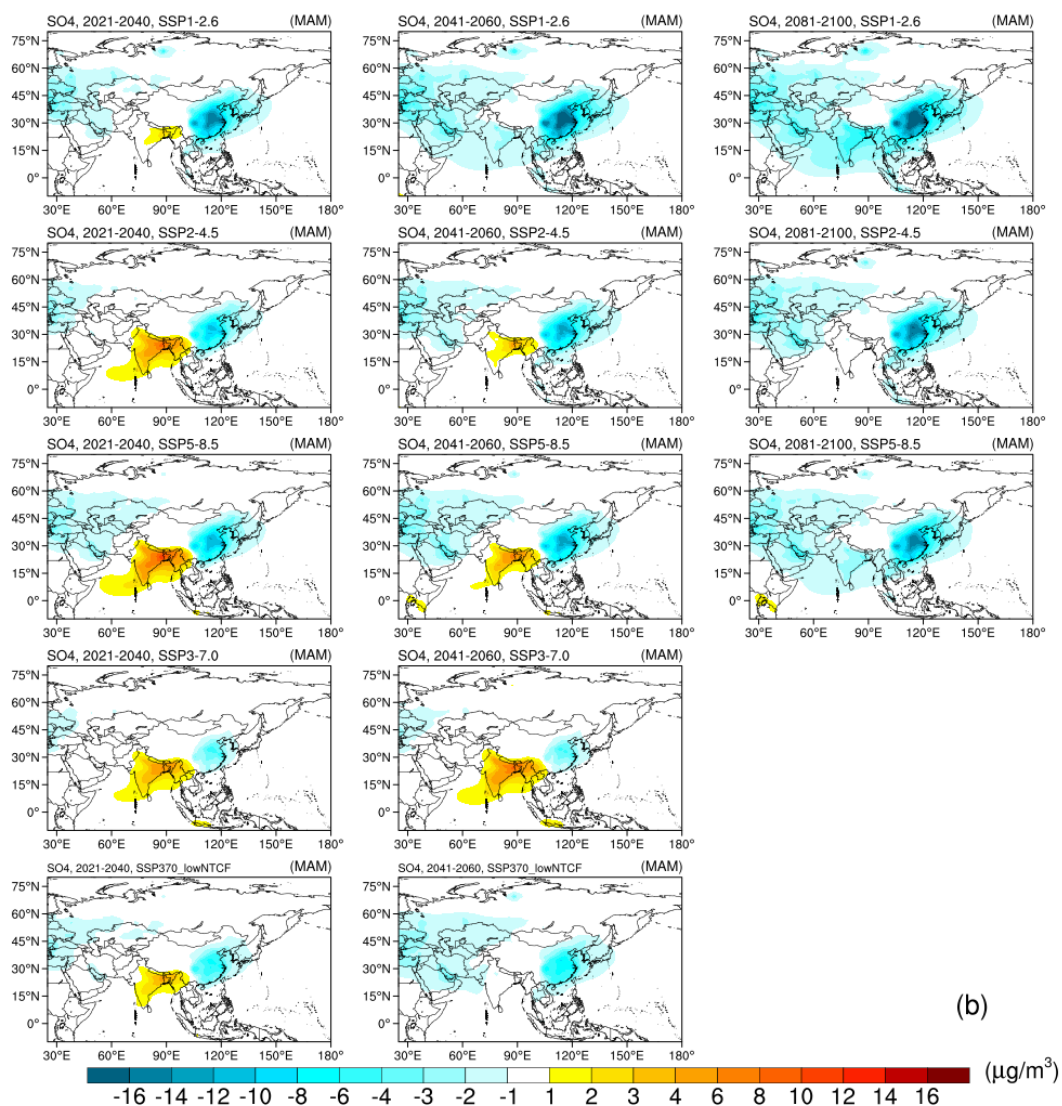
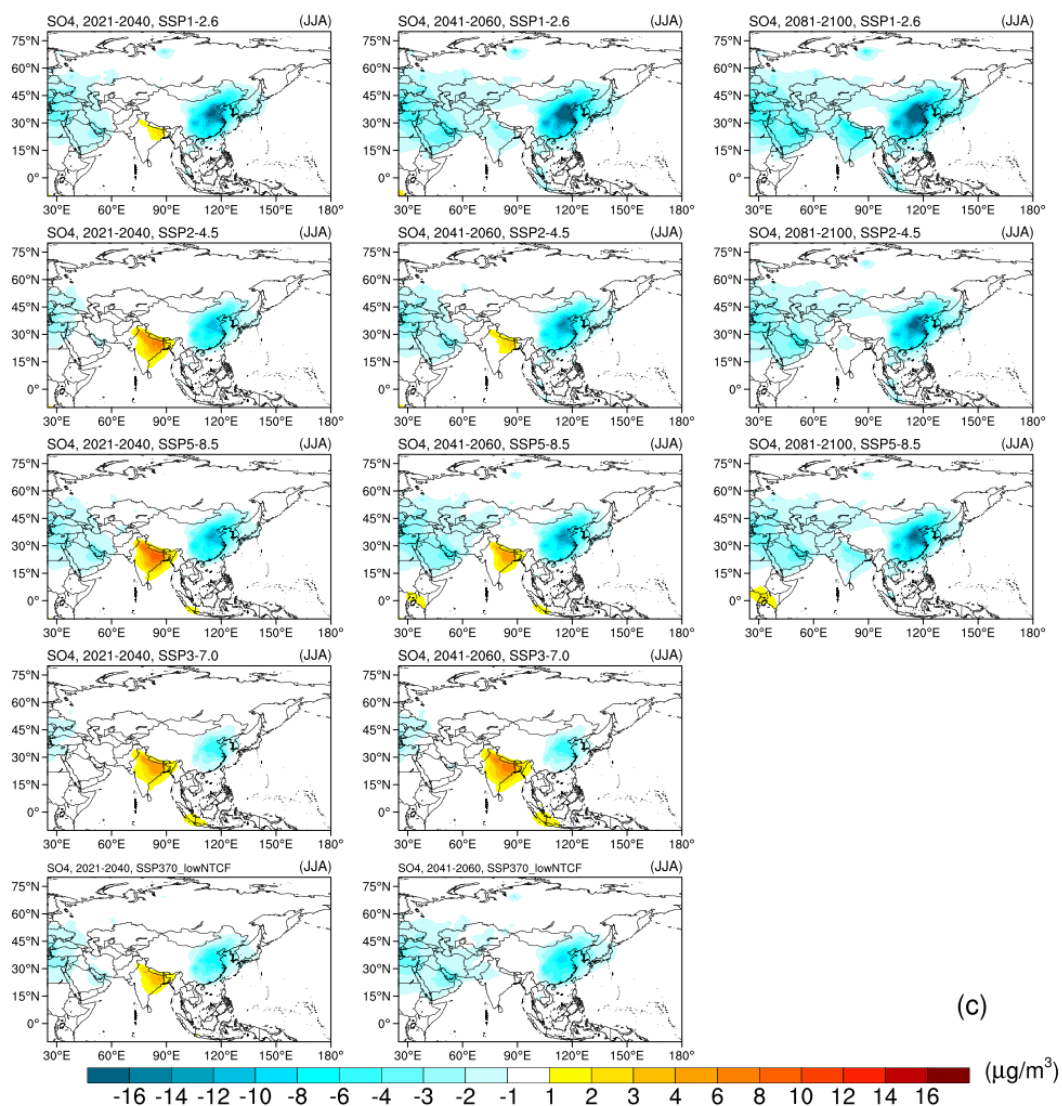


Figure S11 Spatial distribution of projected changes in surface dust concentrations in annual (a), spring (b), summer (c), autumn (d) and winter (e) (units: $\mu\text{g}/\text{m}^3$) during 2021–2040, 2041–2060 and 2081–2100 under SSPs, relative to 1995–2014.

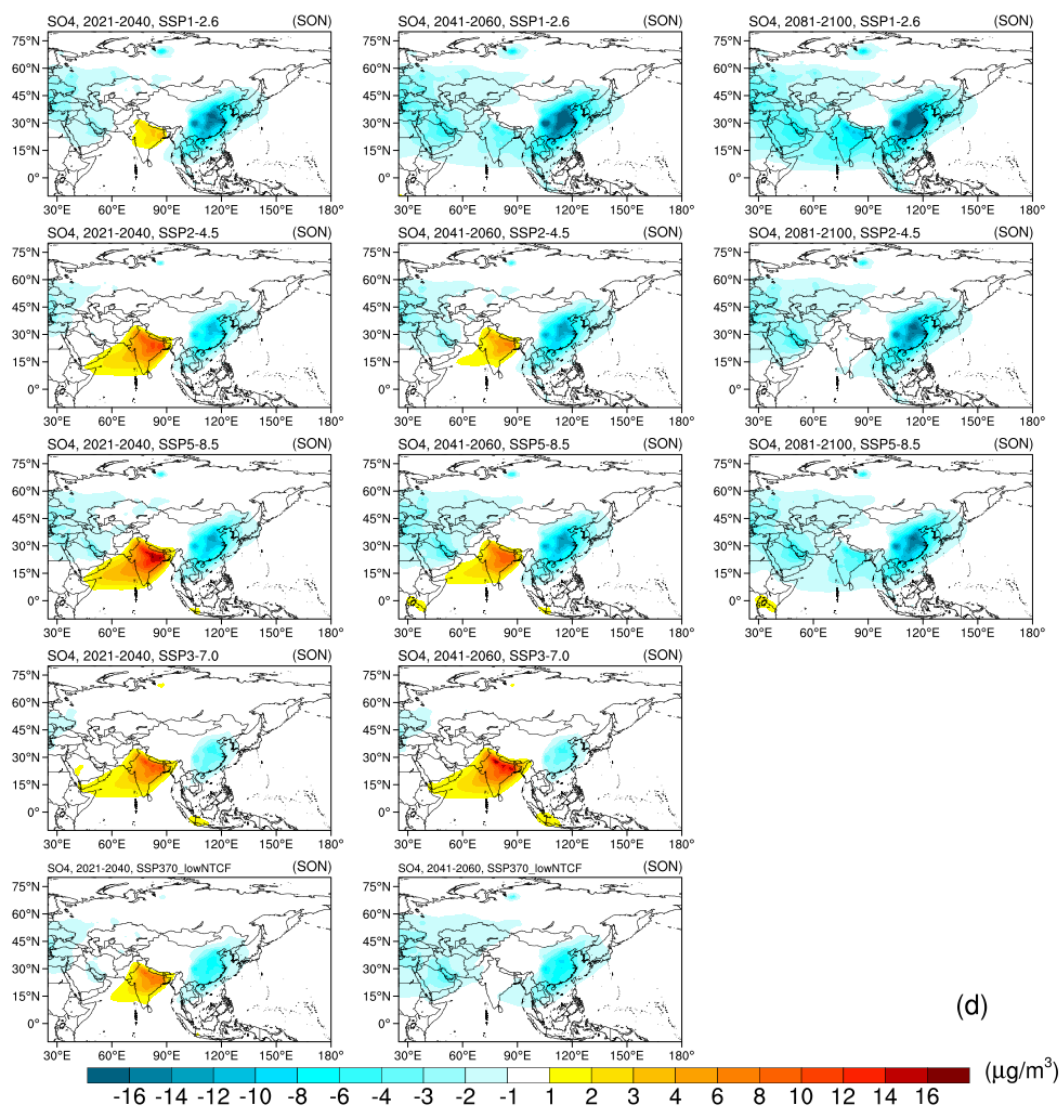


(a)





(c)



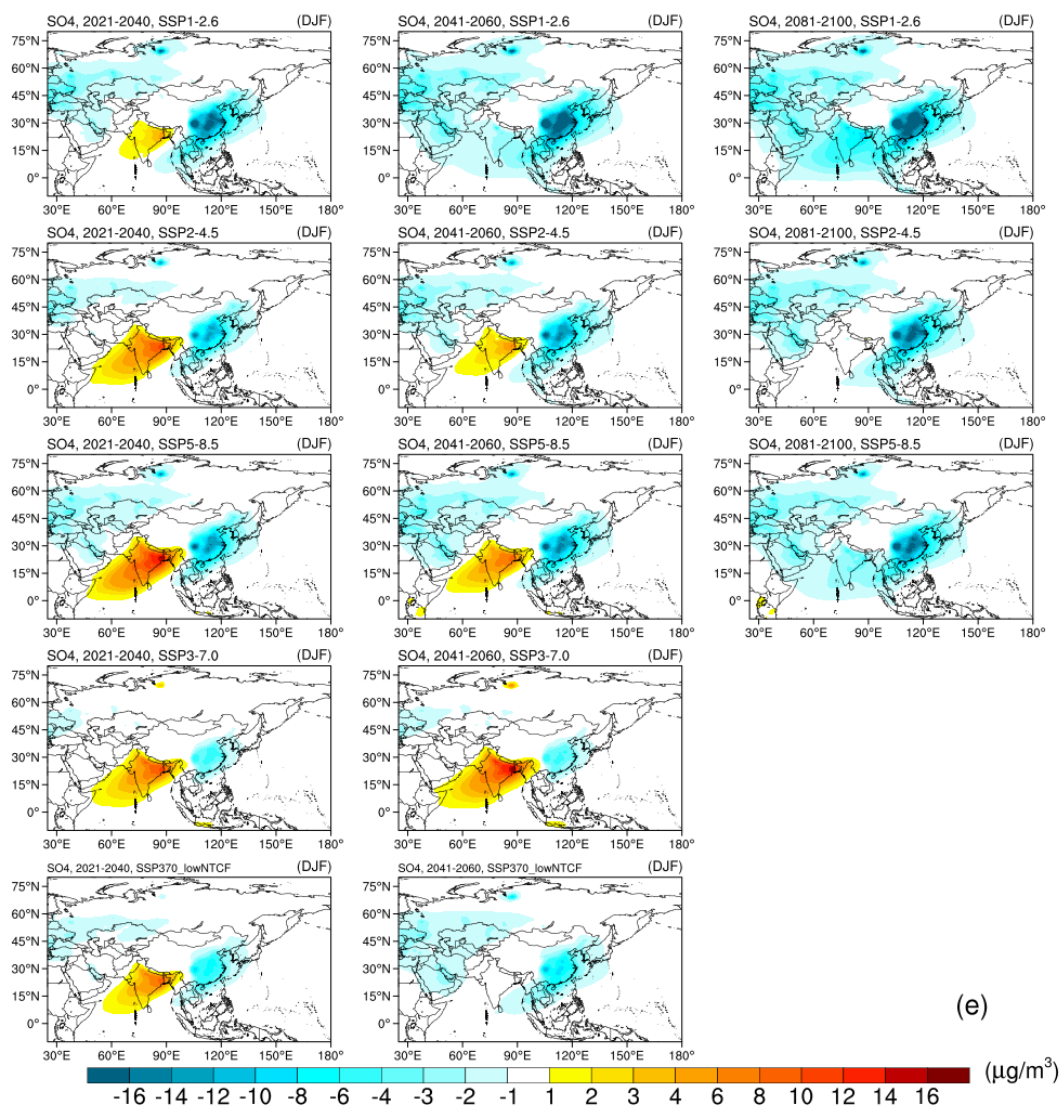
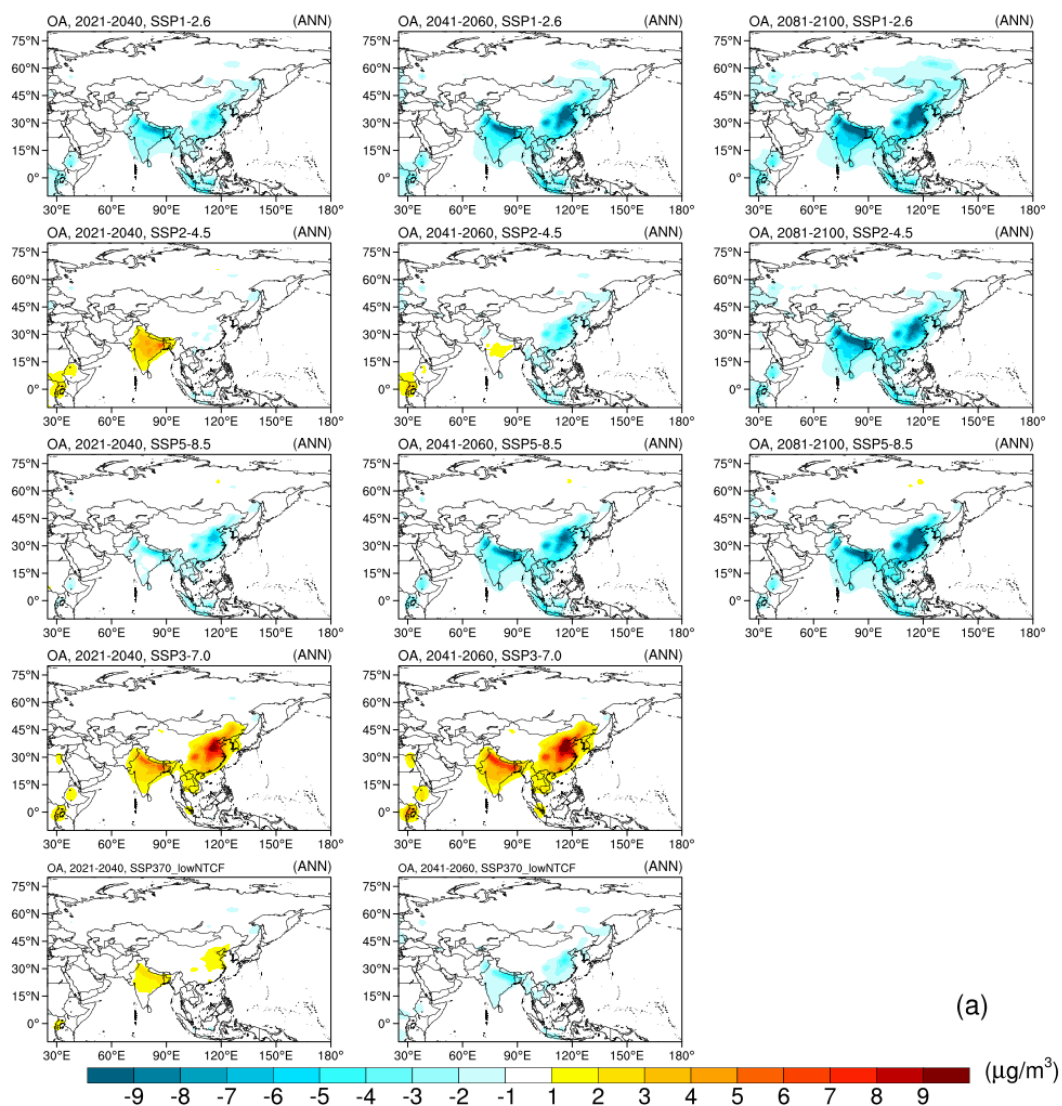
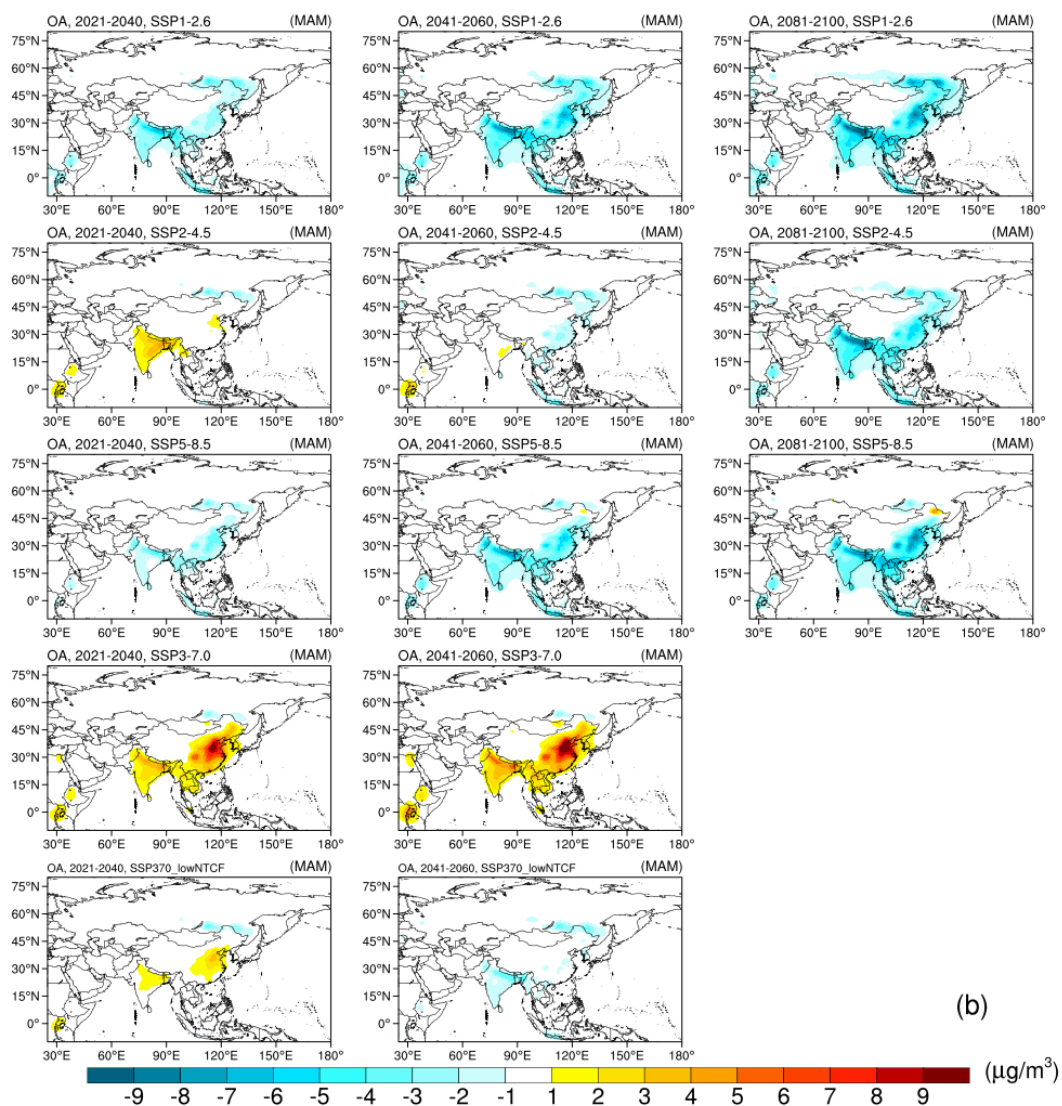
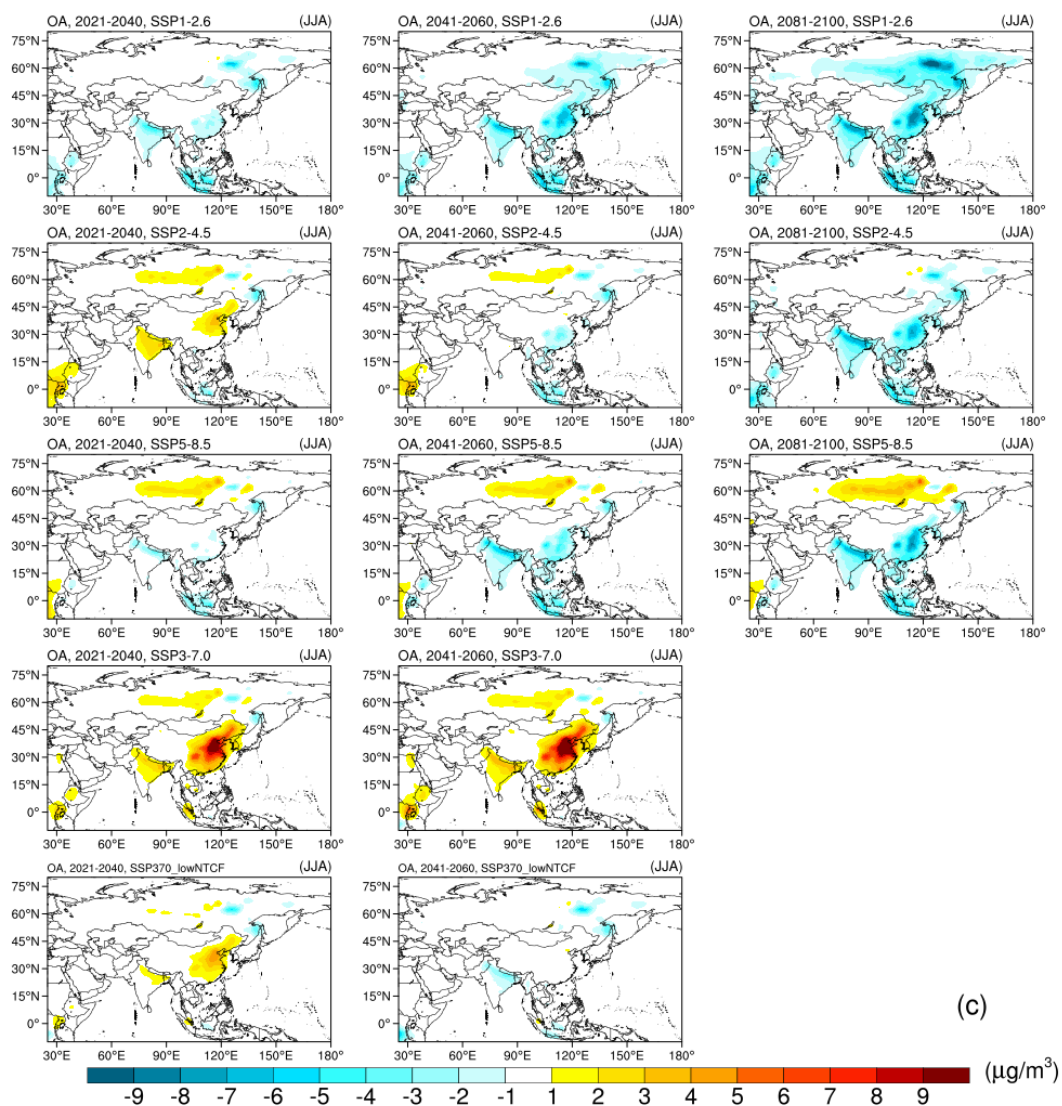


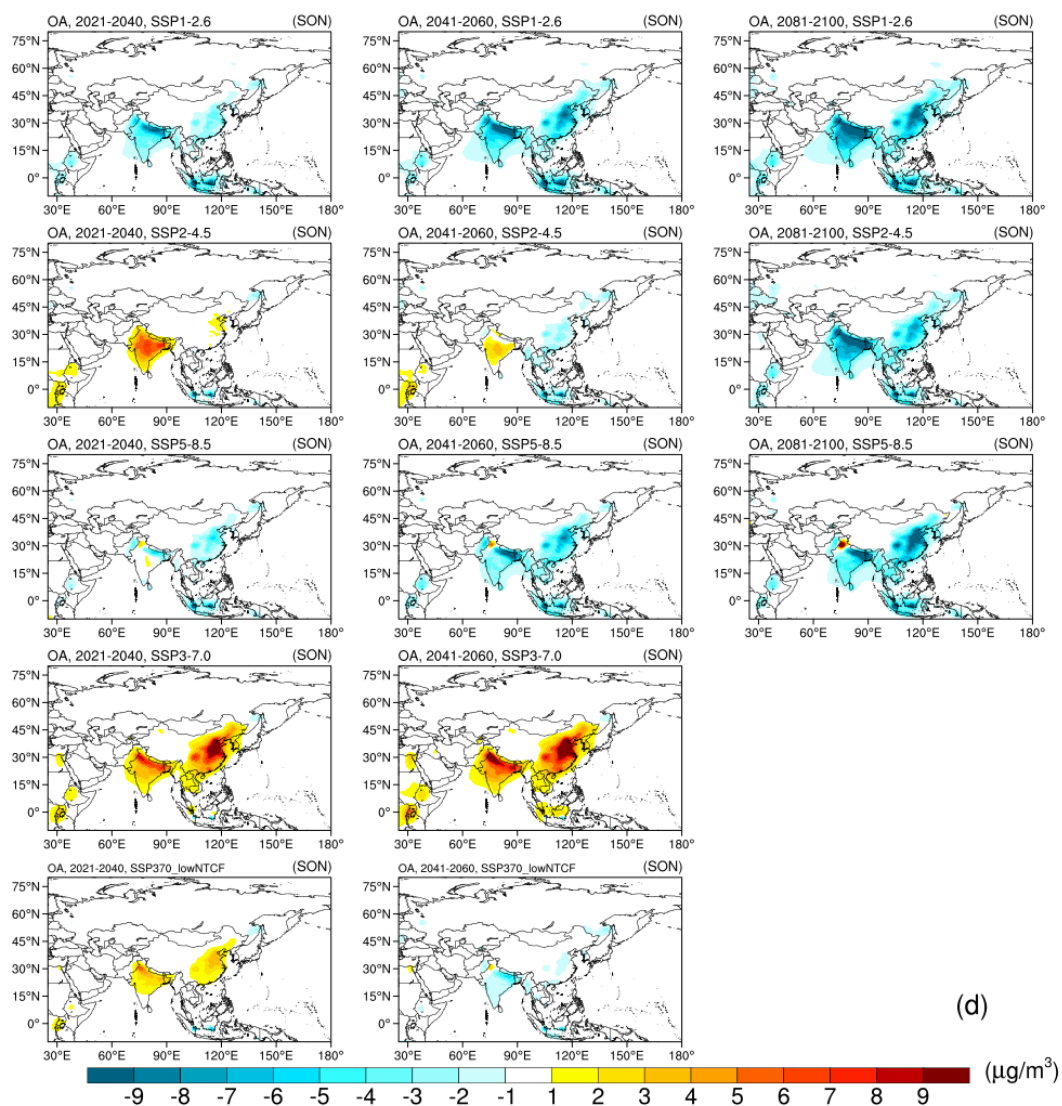
Figure S12 Spatial distribution of projected changes in surface OA concentrations in annual (a), spring (b), summer (c), autumn (d) and winter (e) (units: $\mu\text{g}/\text{m}^3$) during 2021–2040, 2041–2060 and 2081–2100 under SSPs, relative to 1995–2014.



(a)







(d)

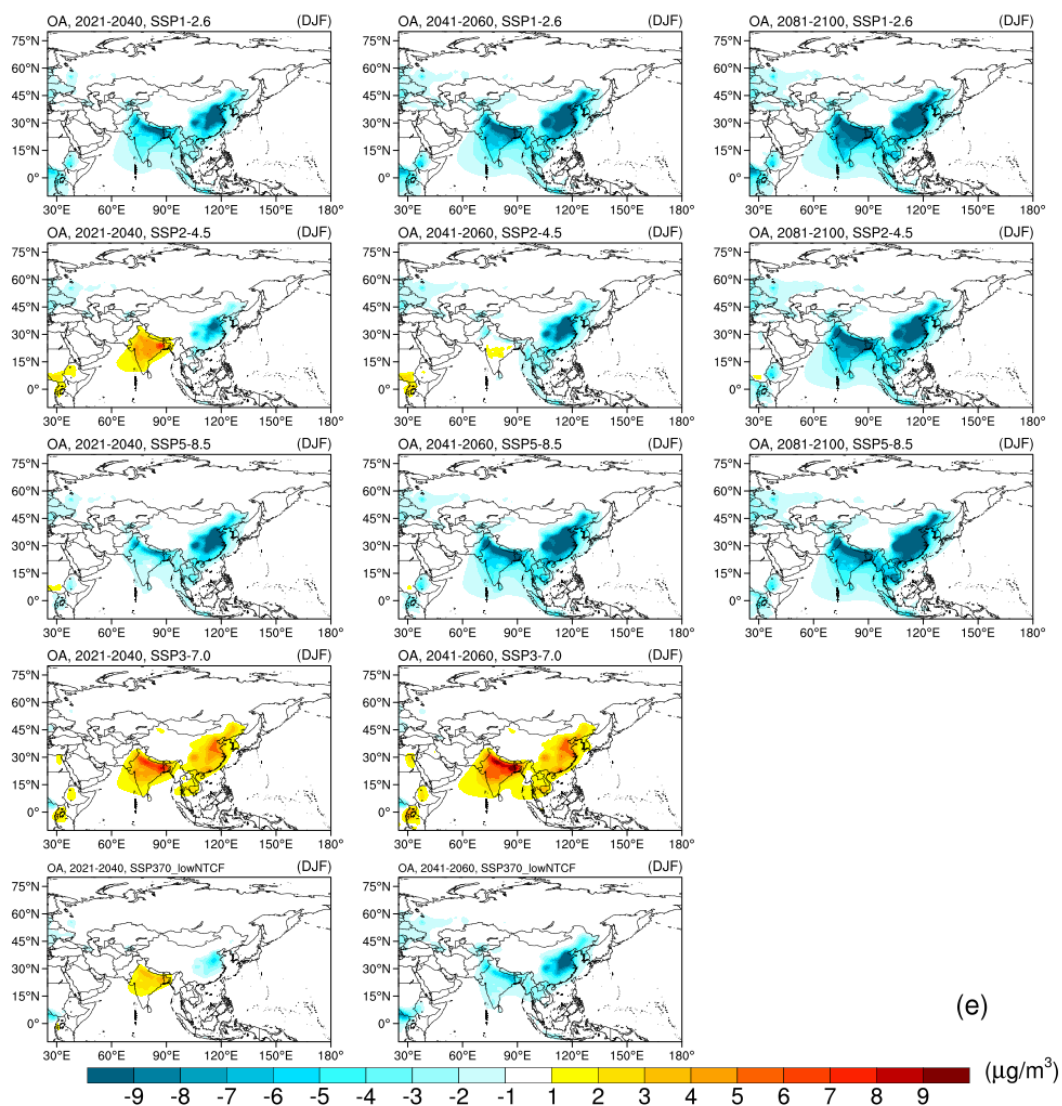
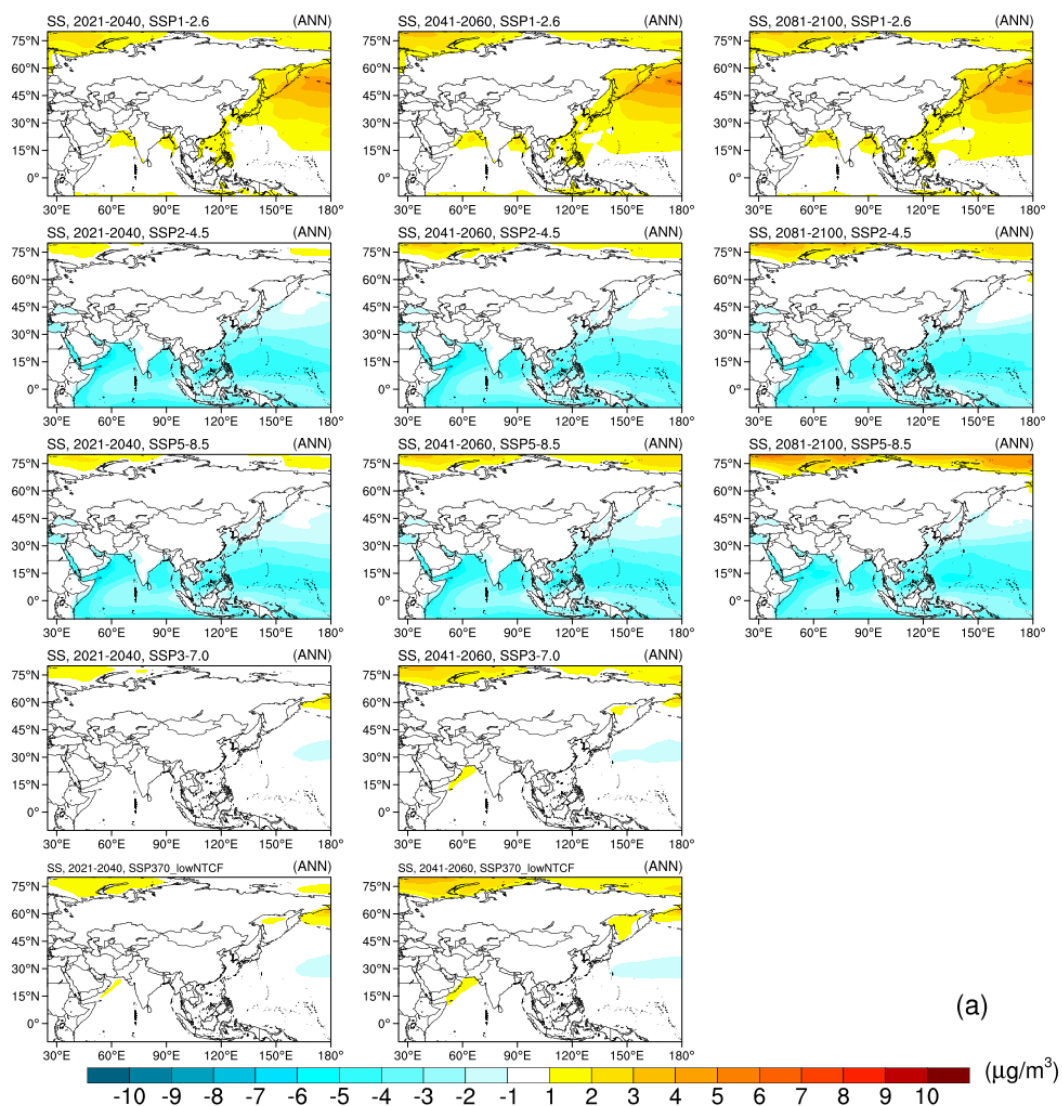
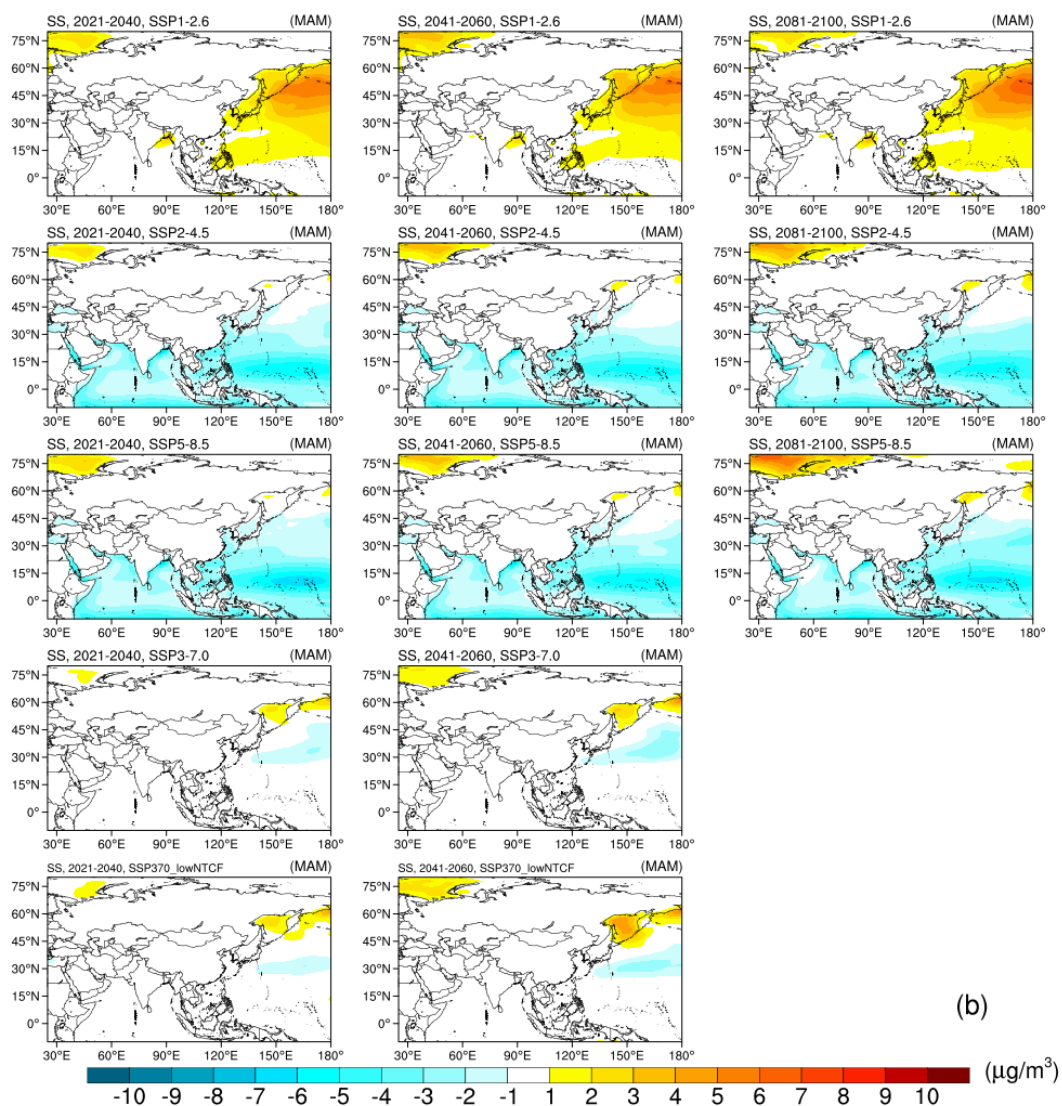
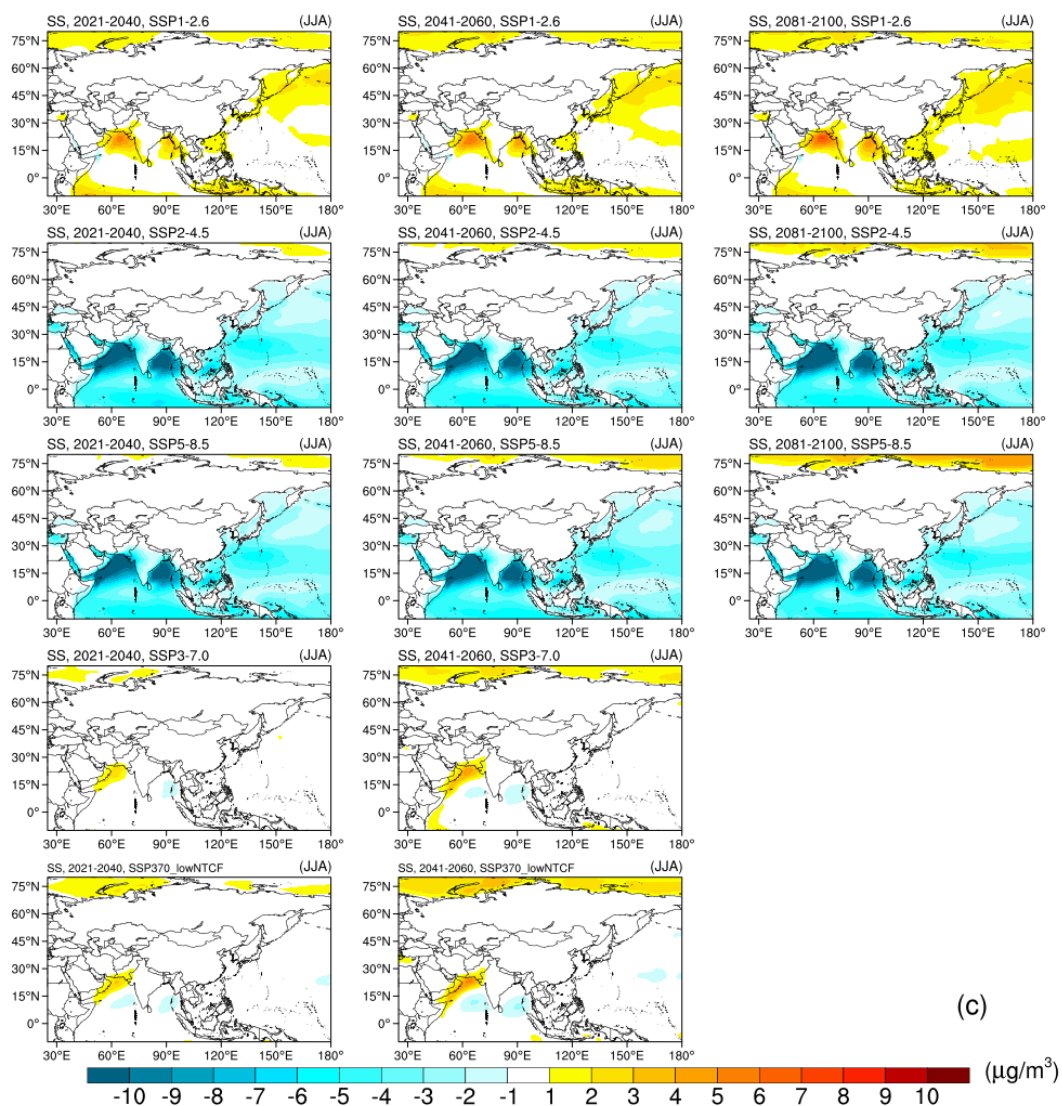


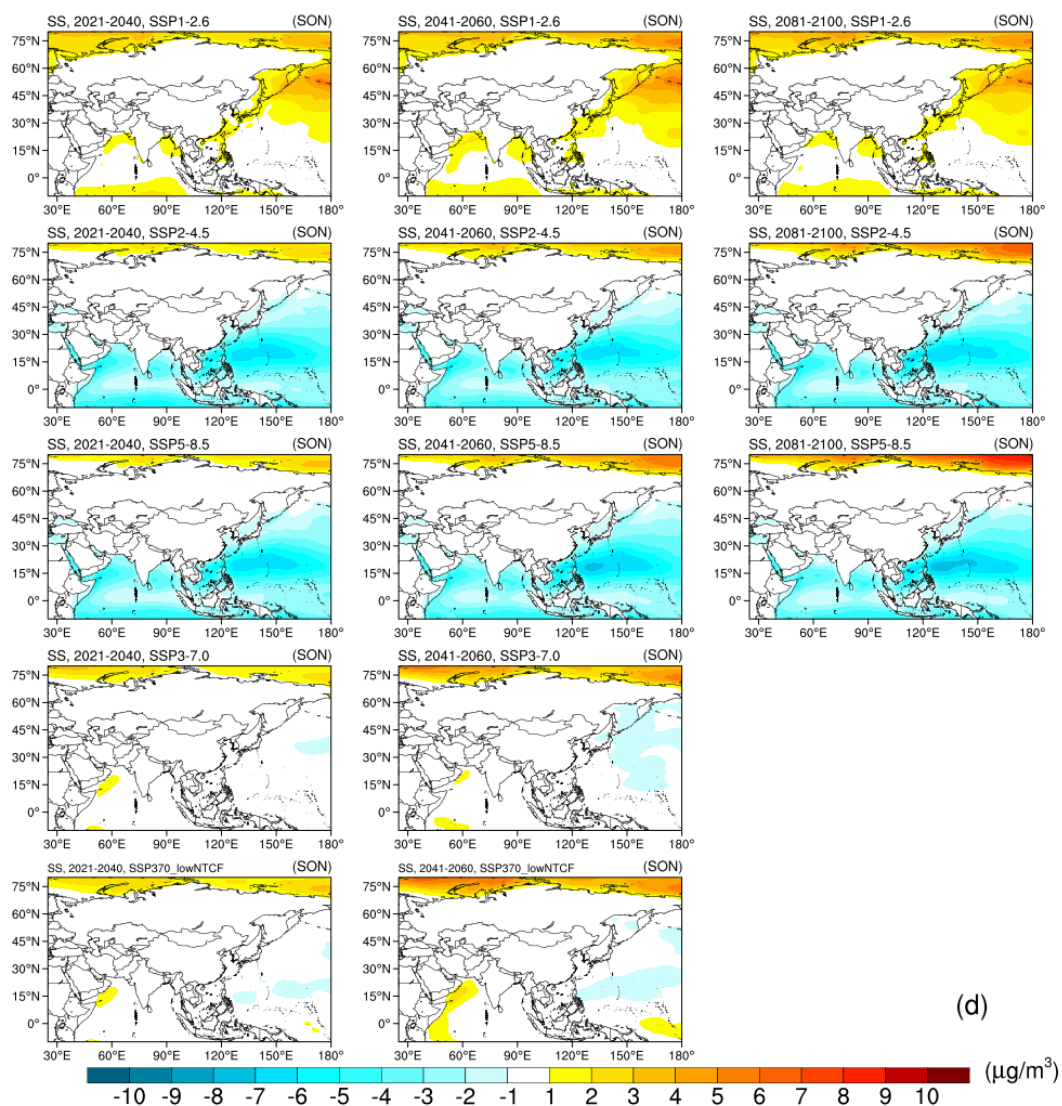
Figure S13 Spatial distribution of projected changes in surface SO_4 concentrations in annual (a), spring (b), summer (c), autumn (d) and winter (e) (units: $\mu\text{g}/\text{m}^3$) during 2021–2040, 2041–2060 and 2081–2100 under SSPs, relative to 1995–2014.



(a)







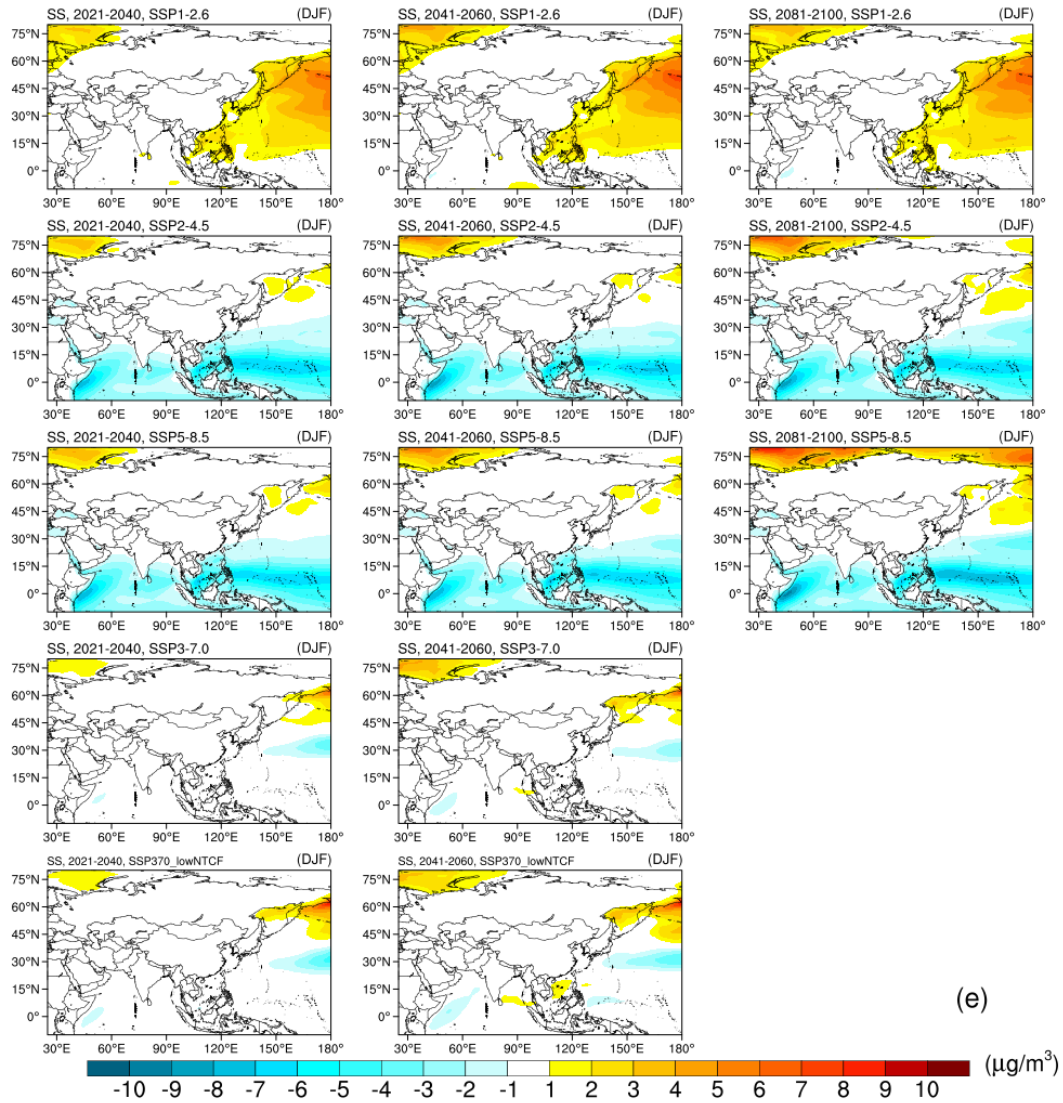


Figure S14 Spatial distribution of projected changes in surface SS concentrations in annual (a), spring (b), summer (c), autumn (d) and winter (e) (units: $\mu\text{g}/\text{m}^3$) during 2021–2040, 2041–2060 and 2081–2100 under SSPs, relative to 1995–2014.